OCTOBER 2018

SAN FRANCISCO ESTUARY & WATERSHED SCIENCE

Sponsored by the Delta Science Program and the UC Davis John Muir Institute of the Environment

RESEARCH

Zooplankton Dynamics in the Cache Slough Complex of the Upper San Francisco Estuary

Wim Kimmerer,*[1] Toni R. Ignoffo,[1] Brooke Bemowski,[1] Julien Modéran,[1] Ann Holmes,[2] and Brian Bergamaschi[3]

Volume 16, Issue 3 | Article 4
https://doi.org/10.15447/sfews.2018v16iss3art4

* Corresponding author: *kimmerer@sfsu.edu*

1 Estuary and Ocean Science Center
San Francisco State University
Tiburon, CA 94920 USA

2 Department of Animal Science
University of California, Davis
Davis, CA 95616 USA

3 California Water Science Center
U.S. Geological Survey
Sacramento, CA 95819 USA

ABSTRACT

We studied abundance and dynamics of zooplankton in the tidal freshwater Cache Slough Complex (CSC) in the northern Delta of the San Francisco Estuary during June, July, and October 2015. We asked whether the CSC was an area of high zooplankton production that could act as a source region for open waters of the estuary. Abundance of the copepod *Pseudodiaptomus forbesi* was similar to that in freshwater reaches of the central and eastern Delta and higher than that in the adjacent Sacramento River. Growth rate of *P. forbesi* was higher than previously measured in large estuarine channels because of higher temperature and phytoplankton biomass in the CSC. Samples of *P. forbesi* examined with molecular techniques contained an unexpectedly high proportion of DNA from cyanobacteria and little DNA from more nutritious phytoplankton. We also examined tidal exchanges of phytoplankton biomass and copepods between Liberty Island, a shallow tidal lake within the CSC, and the adjacent southern Cache Slough, which links the CSC to the Sacramento River. We calculated zero net flux of phytoplankton over 127 days between June and October. The tidal flux of copepods, calculated using tidal flow from an in situ flow station and half-hourly sampling over three 24.8-hr tidal cycles, varied a great deal because of temporal patchiness and day/night variation in abundance. Overall, the tidal flux was indistinguishable from zero, while the tidally averaged water flow (and therefore the net copepod flux) was always into the wetland. Our results show some promise for the CSC as a productive habitat for planktivorous fishes and as a laboratory for learning how to design future wetland restoration. However, we remain cautious about whether wetlands such as the CSC may export large quantities of food organisms that can support fishes in other regions of the estuary.

KEY WORDS

Wetland, productivity, planktivorous fish, copepod, *Pseudodiaptomus forbesi*, growth rate, tidal exchange

INTRODUCTION

Wetlands are productive elements of natural landscapes with many attributes valued by human populations. They can support productive food webs and species of concern, improve water quality, sequester carbon, protect shorelines, and provide opportunities for active and passive recreation (Zedler and Kercher 2005). About half of the world's wetland area has been lost to human encroachment, and a realization of their value has led to increasing efforts at restoration (Zedler and Kercher 2005). In the San Francisco Estuary (estuary) about 95 % of the total wetland area has been lost, mainly to development starting over a century ago (Nichols et al. 1986). The high value of the lost wetlands has been inferred from analogues elsewhere and from the function of small remnant wetlands (e.g., Grimaldo et al. 2009).

Wetlands provide habitat for a variety of fish species and life stages, which occupy the habitat as residents or transients, or for rearing (Kneib 1997). The habitat value of wetlands arises from the shelter provided by complex bathymetry, turbidity, and aquatic vegetation, and from the high productivity of food sources for fish. Food sources within wetlands may include insects, benthic fauna, fauna resident on surfaces such as vegetation, and zooplankton, which are typically consumed mainly by small forms, including larval and early juvenile fishes.

Interest in the restoration of tidal wetlands in the California Delta has arisen because of their potential to enhance food supply for declining species of pelagic fish, notably Delta Smelt (*Hypomesus transpacificus)* (Herbold et al. 2014). Delta Smelt, and probably other fishes in the estuary, are food limited, meaning that a greater abundance of their zooplankton prey would increase smelt population size through faster growth and higher reproductive rate (Kimmerer and Rose 2018). Food limitation of Delta Smelt is suggested by analyses of gut fullness (Nobriga 2002; Slater and Baxter 2014), glycogen depletion (Bennett 2005; Hammock et al. 2015), reduced size at age (Bennett 2005), statistical relationships of food to survival indices (Kimmerer 2008), and functional responses measured in the laboratory that show low feeding rates at current levels of prey abundance (Sullivan et al. 2016).

The summer–autumn habitat of Delta Smelt has historically been the Low-Salinity Zone (LSZ), where salinity, temperature, and turbidity are suitable (Bennett 2005; Nobriga et al. 2008; Kimmerer et al. 2013). However, conditions in the LSZ have deteriorated, with declines in turbidity, primary production, and zooplankton abundance (Cloern and Jassby 2012; Kimmerer and Thompson 2014). The freshwater Cache Slough Complex (CSC; Figure 1) in the northern Delta has attracted the attention of scientists and managers because it has provided habitat for some fraction of the Delta Smelt population year-round, at least in recent years (Merz et al. 2011; Sommer and Mejia 2013). This implies that the CSC is an alternative habitat to the LSZ, potentially mitigating the risk of population crashes if conditions in the LSZ deteriorate further. It also suggests that restoration of additional habitat in the north Delta may benefit Delta Smelt directly, or that elevated food web productivity may support the export of zooplankton from the wetland, thereby subsidizing the food web of the broader estuary (BDCP 2014; Herbold et al. 2014).

Summer daytime water temperature in the CSC is often higher—and salinity lower—than in the areas where Delta Smelt are most often caught (temperature ~20–24 °C, salinity ~0.5–6; Feyrer et al. 2007; Nobriga et al. 2008; Sommer and Mejia 2013). Physiologically stressful conditions (e.g., temperature; Komoroske et al. 2015) may impose energetic penalties that could be offset by high feeding rates (Brown et al. 2004). Higher abundance of the zooplankton prey of Delta Smelt in the CSC and elevated turbidity (Morgan–King and Schoellhamer 2013) that reduces the risk of foraging may contribute to high feeding rates. Gut fullness of Delta Smelt was elevated at salinity <0.55 in summer compared to values at higher salinity, although it was depressed in fall and winter (Hammock et al. 2017).

We assessed the food resources available to Delta Smelt and other fishes in the CSC during summer–autumn 2015. We determined abundance (number per m^{-3}) of zooplankton, particularly the numerically dominant copepod *Pseudodiaptomus forbesi*, which made up at least half of the diet of juvenile Delta Smelt in 2005–2006 (Slater and Baxter 2014) and in the CSC in 2010 and 2011 (IEP 2015), and more than half in the diets of various larval fishes in

the CSC in May 2015 (2016 poster presented by E. Howe, unreferenced, see "Notes"). *Pseudodiaptomus forbesi* was by far the most abundant zooplankton in our study (see "Results"). We measured the growth rates of copepodites (juveniles) of this species and compared them with values previously determined in the LSZ and freshwaters of the western Delta. We obtained information on feeding by *P. forbesi* from stable isotopes of carbon and nitrogen, and from DNA-based identification of phytoplankton in the water and in the copepods. Finally, we measured the flux of phytoplankton and copepods through the southern entrance of Liberty Island to assess the likelihood that plankton biomass produced within the CSC could be exported to nearby estuarine channels.

METHODS

Study Site and Species

The CSC (Figure 1) is an extensive network of remnant and restored wetlands, tidal channels, and tidal lakes in the northern Delta. The CSC is geographically and hydrodynamically complex, with areas of emergent vegetation, shoals, and deep channels; tidal currents that mix and transport organisms, nutrients, and other substances; and a spatial gradient of water age and phytoplankton biomass (Downing et al. 2016). This complexity likely contributes to the suitability of the CSC as habitat for fish (Moyle 2008) by providing foraging sites close to refuges from predation. In addition, blooms of the toxic cyanobacterium *Microcystis aeruginosa*

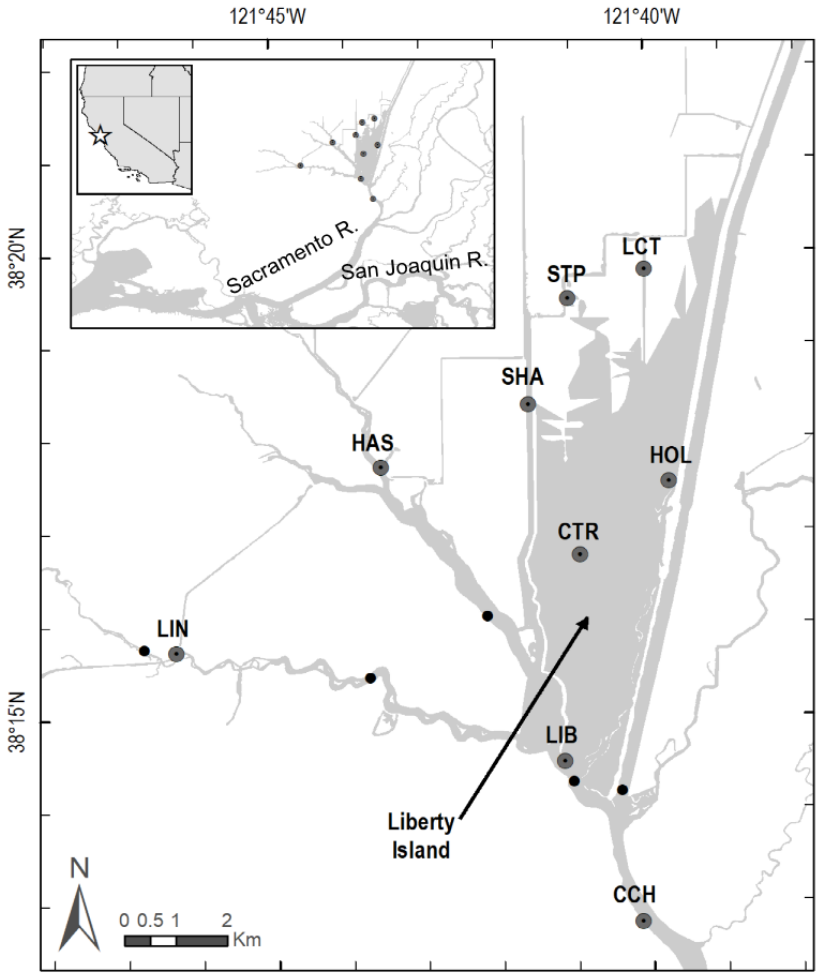

Figure 1 Map of the Cache Slough Complex (CSC) in the northern California Delta. Large circles indicate sampling stations (Table 1), and smaller circles indicate monitoring stations from which data were taken for comparison.

https://doi.org/10.15447/sfews.2018v16iss3art4

(Hammock et al. 2015) are less common in the CSC than in other areas of the Delta, and invasive plants that choke the waterways of the central Delta are also less abundant in the CSC, though their extent has been increasing (2018 email from S. Khanna, CDFW, to W. Kimmerer, unreferenced, see "Notes").

The calanoid copepod *P. forbesi* was introduced to the estuary in 1986 from subtropical to tropical regions of the Asian continent (Orsi and Walter 1991). It has since been abundant in freshwater (Kimmerer et al. 2017) and a key food for planktivorous fishes (Hobbs et al. 2006; Bryant and Arnold 2007; Slater and Baxter 2014). This species has also been introduced to the Columbia River Estuary, probably through coastal shipping from the San Francisco Estuary (Cordell et al. 2008). This estuarine copepod is demersal: during daytime, the late copepodite and adult stages remain on the bottom in shallow or clear water, migrating into the water column at night (Kimmerer and Slaughter 2016), though not in the more turbid, deep channels of the estuary (Kimmerer et al. 2002).

Abundance and Distribution

We collected data during three 1-week sampling periods in June, July, and October 2015 using the research vessel (R/V) Mary Landsteiner. During each sampling period, we collected zooplankton and microplankton to determine abundance, measured copepod growth rate and the flux of copepods in and out of Liberty Island, and took samples for genetic analysis of feeding and stable isotope analysis. Each week's study began with a daytime transect throughout the CSC, where we collected data with sensors to measure chlorophyll fluorescence, turbidity, temperature, and conductivity, while underway at high speed, as described by Downing et al. (2016). During the transects, we stopped at 10 stations (Figure 1, Table 1) for discrete samples. Zooplankton samples were taken in June with a 150-µm-mesh, 50-cm-diameter conical net equipped with a flow meter and towed just below the surface. Samples were preserved in 2–5% formaldehyde. To improve collection of copepod nauplius larvae, we used a 53-µm-mesh net in the July and October sampling; all other procedures were the same. We repeated transects on the second and fourth day of each sample period to replicate samples taken at the 10 discrete stations.

At each station, water samples were collected from just below the surface and stored in amber glass bottles with acid Lugol's solution for counts of microplankton. Additional water samples were filtered onto 5-µm Nuclepore filters and GF/F (glass fiber filters; Whatman®, ~0.7 µm) for chlorophyll analysis. The 5-µm-size fraction was analyzed because copepods can feed more efficiently on larger cells than on smaller ones (Paffenhöfer 1984), and the proportion of larger cells in the northern estuary has declined (Kimmerer et al. 2012).

Table 1 Station names, labels, locations, and characteristics. Stations are arrayed north to south (Figure 1). Depth and turbidity are means of measurements during sampling. Z01:Depth is the ratio of the 1% light level to water depth, based on turbidity values and a relationship of turbidity to light extinction coefficient calculated from IEP water quality monitoring data, 2000–2012: k = 0.52 + (0.126 ± 0.007) Turbidity, N = 432.

Station name	Label	N Lat.	W. Long.	Depth, m	Turbidity, FNU	Z01: Depth	Characteristics
Liberty Cut	LCT	38.330	121.667	5.0	29	0.3	Artificial channel, quiescent; forest
Stairstep	STP	38.325	121.684	5.5	24	0.3	Narrow, shallow channel, quiescent; forest
Shag Slough	SHA	38.306	121.693	6.7	29	0.2	Artificial channel; agriculture and forest
Little Holland Tract	HOL	38.292	121.662	1.3	19	1.9	Small wetland by channel; forest
Haas Slough	HAS	38.295	121.726	3.7	36	0.5	Natural slough with riprap, energetic; agriculture
Liberty Island Center	CTR	38.279	121.682	1.5	10	1.9	Center of tidal lake
Lindsey Slough	LIN	38.262	121.772	4.3	3	1.2	Natural slough with riprap; agriculture
Liberty Island South	LIB	38.242	121.686	4.2	5	1.0	Main opening of tidal lake, energetic
Cache Slough	CCH	38.213	121.669	13.1	7	0.3	Large tidal channel north of confluence with Sacramento River, energetic

In the laboratory, zooplankton samples were rinsed with freshwater and one or more sub-samples were taken with a piston pipette to obtain at least 200 organisms and at least 140 *P. forbesi*. Sub-samples were counted under a dissecting microscope, and counts converted to numbers m^{-3}. We analyzed chlorophyll by extracting filters in 90% acetone and measuring fluorescence using a Turner Designs 10-AU benchtop fluorometer calibrated with pure chlorophyll (Arar and Collins 1997). Chlorophyll data from the GF/F filters were used to calibrate underway fluorescence measured in the field to total chlorophyll, separately, for each sampling period. To link underway data to station data, we took medians of underway data points taken within 1 km of each sampling station (median 50, range 10–392 data points). The same link was used to determine median turbidity at the sampling stations.

Samples preserved in Lugol's solution were gently agitated, then a 50-ml sub-sample was poured into a conical centrifuge tube and allowed to settle for at least 8 days. The supernatant liquid was decanted off, and the remaining sample was re-suspended and examined with a Wild M40 inverted microscope. We examined either the entire sub-sample or randomly selected fields for microplankton; here, we use counts of microzooplankton only. We measured the more abundant cell types in representative sub-samples, calculated estimates of volume using elliptical shapes, and calculated carbon mass using a mass density of 0.19 pg C µm-3 (Putt and Stoecker 1989).

We obtained additional zooplankton abundance data from three long-term fish-monitoring programs to provide a broader spatial and temporal context to our data. These programs, run by the California Department of Wildlife (CDFW) for the Interagency Ecological Program (IEP), also collect zooplankton: the spring 20-mm survey (Dege and Brown 2004), Summer Townet Survey (TNS; Turner and Chadwick 1972), and fall Midwater Trawl Survey (FMWT; Moyle et al. 1992). Complete data sets and meta-data are available from CDFW (*https://www.wildlife.ca.gov/Conservation/Delta*, accessed January 22, 2018). We used data from 2008 (2011 in the fall survey) to 2015 for abundance of *P. forbesi* copepodites and adults. Data were aggregated as geometric means with confidence intervals for June, July, and October of each year by region: the CSC (all in the southern end of the CSC, Figure 1), the LSZ (salinity 0.5 to 6, not including stations in the eastern Delta), between the confluences with Cache Slough and the San Joaquin River (at salinity <0.5 in the lower Sacramento River), and in the Delta south of the Sacramento River and east of the LSZ. We excluded the easternmost station (919, 38°06.3′N, 121°29.7′W), which had anomalously low abundance compared to those of the other stations, probably because of demersal vertical migration (Figure 11; Kimmerer and Slaughter 2016).

Growth and Feeding

We determined somatic growth rates of copepods at three stations using a modification of the artificial cohort method (Kimmerer and McKinnon 1987). We collected live copepods by gentle subsurface tows with a 150-µm-mesh net and size fractionated the samples between 200 and 224 µm. The selected size fraction usually contained early copepodites, although nauplii were abundant in two samples, requiring additional calibration as discussed below. We diluted the size fraction into ~18 L of surface water, then repeatedly mixed and sub-sampled with a beaker sized to obtain ~160 copepods per subsample. We poured sub-samples alternately into sample jars and 4-L cubitainers® filled with surface water. We preserved six initial sub-samples in jars for analysis in 2% glutaraldehyde, which minimizes changes in volume and mass during preservation (Kimmerer and McKinnon 1986). Ten cubitainers were capped and suspended for incubation attached to a float at the Liberty Island site (LIB; Figure 1) to maintain near-ambient temperature and some water motion. After incubation for 2 and 3 d, we removed five cubitainers and preserved contents as above.

Best practice suggests that the artificial cohort method should be applied using the mean or median mass (as dry weight or carbon) of the copepods in each sample (Kimmerer et al. 2007). Since this practice is very labor-intensive, we modified the method by using image analysis as an efficient proxy for mass per copepod (Alcaraz et al. 2003). We imaged sub-samples on a Leica M125 dissecting microscope with a Spot Idea S8APO digital camera. First, we arranged a sub-sample of 30–100 copepods, held in preservative for at least a month, on the tray

https://doi.org/10.15447/sfews.2018v16iss3art4

so their images would not overlap. Then, we took measurements with an automated protocol developed using ImageJ scientific-imaging freeware. Since copepods are roughly the shape of an ellipsoid, we used measurements of the major and minor axes of the copepods to calculate their volumes (Alcaraz et al. 2003).

We calibrated copepod volumes to carbon mass using copepods collected on August 3, 2016 at station LIB (Figure 1) by a gentle subsurface tow with a 53-µm-mesh net. We fixed and held the sample in 2% glutaraldehyde as for the incubated samples, then rinsed the copepods with Milli-Q water and sorted by life stage from the sample. We obtained triplicate samples of stages from nauplius stage 4 to copepodite stage 4, and copepodite stage 5 and adults separately, by sex. On average, we examined between 35 (adult females) and 120 (nauplius 4) copepods. We took duplicate images of all copepods in each sample as described above. We then placed copepods from each sample in pre-weighed tin capsules (Costech, 8×5 mm, weighed with a Sartorius SE2 Ultra Microbalance). Capsules were dried at 50°C for 48 h, weighed again, and analyzed for carbon content by the UC Davis Stable Isotope Facility. Carbon data gave a tighter calibration than dry weight, so we used carbon only.

During calibration, it was apparent that the relationship of log ellipse volume to log carbon per copepod was linear within the copepodites, but that the slope changed during metamorphosis from nauplius to copepodite. Therefore, the calibration equation was determined as a broken-line function of log carbon vs. log volume with two linear segments (function "segmented.lm in R v. 3.4.2," R Development Core Team 2015). The calibration had a residual standard error of 0.135, corresponding to an error of 14% in raw carbon values. However, analysis of variance of the log of volume by stage had a mean square error of 0.004, while that of carbon was 0.01, indicating that volume estimates were more precise than carbon estimates, and therefore growth rates would be more precisely estimated from calibrated volume than from carbon measured directly.

Volume per copepod from the artificial-cohort samples was converted to carbon mass using the calibration, and growth rate was calculated as the slope of log carbon vs. time. In three of nine samples the slope changed between the first incubation interval of 0–2 days and the second from days 2 to 3 (analysis of covariance), and for those experiments we used only the initial and 2-day time points to determine growth rate. Growth rates were higher than expected from previous measurements in the estuary (Table 3), and a shorter incubation time was probably warranted.

For comparison with other studies, we corrected growth rates to a temperature of 22°C, at which a previous laboratory study of growth had been conducted (Kimmerer et al. 2017). We used the 72-hr mean temperature recorded at the incubation station LIB as the experimental temperature; daily temperature ranges were ~1°C. The correction used an exponential fit of egg development time to temperature for this species (Sullivan and Kimmerer 2013); typically, development times of eggs and well-fed developing stages of copepods vary similarly with temperature (Corkett and McLaren 1970). Growth rate generally varies inversely with development time, although their temperature coefficients are slightly different (Forster et al. 2011), which should not matter for our study, given the small range of temperature (Table 2). Growth rates corrected to 22 °C were related separately to chlorophyll concentration and to microzooplankton biomass by fitting a rectangular hyperbola (Holling 1966) using function nls (R version 3.4.6). We also calculated the growth rate at each collection station based on the median temperature recorded during the three transects; this value represents the growth rate that would have been expected at each station (Table 2).

Using high-throughput genetic sequencing (Holmes 2018), we determined the phytoplankton consumed by copepods. Here, we summarize the results of that study. Samples were taken during the transects at stations where *P. forbesi* was abundant across a range of chlorophyll values as determined by fluorometry. Copepod samples were taken by net tow as for growth rates, concentrated, preserved in 95% molecular-grade ethanol, and placed on dry ice. Seston samples were filtered onto 1-µm-pore polycarbonate filters (Whatman®) and immediately frozen in liquid nitrogen or dry ice.

Table 2 Growth rates by month and station with 95% confidence intervals (CIs). Growth rates are given as measured, adjusted to 22 °C for comparison with other studies, and adjusted to temperature at the collection site. Stations are arrayed north to south for each sampling date. The maximum days for incubation were nominally 3, but data were cut off at 2 days when the growth rate differed between 0–2 and 2–3 days (Figure 6). N is the total number of samples used to calculate growth rate. The laboratory maximum growth rate for early copepodites was 0.51 ± 0.05 d^{-1} (95% CI; Kimmerer et al. 2017).

Start Date (2015)	Station	Temperature, °C		Max days	Growth rate, d^{-1}			Ratio to laboratory maximum	N
		Collection	Incubation		Measured	T = 22°C	T = Collection		
6 June	LCT	23.3	22.8	2	0.39 ± 0.05	0.35 ± 0.05	0.41 ± 0.06	0.53	11
	HOL	23.5		3	0.32 ± 0.09	0.29 ± 0.08	0.34 ± 0.10	0.33	16
	LIB	23.7		3	0.33 ± 0.05	0.29 ± 0.05	0.36 ± 0.06	0.53	15
28 July	LCT	24.9	23.7	3	0.53 ± 0.05	0.43 ± 0.04	0.61 ± 0.05	0.71	16
	HOL	24.3		3	0.23 ± 0.07	0.19 ± 0.06	0.25 ± 0.08	0.35	16
	LIB	24.2		3	0.27 ± 0.02	0.22 ± 0.02	0.28 ± 0.02	0.29	16
6 October	LCT	20.3	20.6	2	0.53 ± 0.05	0.63 ± 0.06	0.51 ± 0.05	1.33	11
	HOL	20.8		3	0.31 ± 0.04	0.37 ± 0.04	0.32 ± 0.04	0.75	16
	SHA	20.4		2	0.24 ± 0.04	0.29 ± 0.05	0.24 ± 0.04	0.57	11

Eight samples of 23 had sufficient adult female copepods to analyze. At each of these sampling events, we collected two or three filter samples, and later selected 12–14 sub-samples of five adult females from each net tow for analysis. We amplified and sequenced a segment of the 16S rRNA gene on an Illumina MiSeq sequencer. Our approach targeted prokaryotes (including cyanobacteria) and phytoplankton chloroplasts, but did not examine non-photosynthetic eukaryote prey such as most ciliates. Sample preparation, sequencing, and post-processing are described in detail in Holmes (2018). For the purposes of this paper, we aggregated cyanobacteria and chloroplast sequences to the phylum level, or to the genus level for two common cyanobacteria. We then calculated the mean proportion of reads in each of these groups across all copepod samples and all filter samples from each sampling event. These were used graphically to examine differences between relative abundance of phytoplankton taxa in the water and in copepods.

We also assessed feeding and trophic structure using stable isotopes of carbon and nitrogen (Peterson et al. 1985) in samples of seston and zooplankton collected on 1 or 2 days of each study period. We collected seston samples on GF/F filters as for chlorophyll, above, and stored on dry ice. Copepod samples were collected by gentle net tows, concentrated in small jars, frozen in liquid nitrogen, and stored on dry ice. In the laboratory, we selected sub-samples of 86–300 (median 200) adults or late-stage copepodites of *P. forbesi* from the samples and placed them in tin cups, as above for carbon analysis. Copepod and seston samples were dried at 50°C for at least 48 h. The Center for Stable Isotope Biogeochemistry at the University of California Berkeley analyzed samples by Continuous–Flow Isotope Ratio Mass spectrometry (CF-IRMS) using an IsoPrime 100 mass spectrometer (Isoprime, Cheadle, UK) interfaced with an elemental analyzer (vario ISOTOPE cube, Elementar, Hanau, Germany). Stable isotope ratios are expressed in standard δ notation (Peterson et al. 1985).

Flux Estimates

We measured the flux of phytoplankton biomass and *P. forbesi* individuals to and from the wetland through its largest channel at the southern LIB station (Figure 1) over three full tidal cycles. A bottom-mounted acoustic Doppler current profiler (ADCP) was in operation at this station and had been calibrated to give flow rate through the cross-section (*https://waterdata.usgs.gov/nwis/uv/?site_no=11455315*, accessed January 26, 2018). Flow data were available at 15-min intervals for June–October. Water quality data were available at the same site for various continuous measurements, including temperature, conductivity, chlorophyll fluorescence, and turbidity; zooplankton samples were taken by pump at half-hour intervals near the ADCP.

https://doi.org/10.15447/sfews.2018v16iss3art4

Material fluxes in a channel can result from net flow (i.e., advection), and from spatial and temporal correlations of concentration with velocity. We assumed that spatial correlations (i.e., cross-sectional and vertical) and higher-order terms (e.g., spatio-temporal correlations) were negligible. The shallow water, strong currents, and lack of stratification at the sample station rule out vertical correlations, such as by gravitational circulation, though they are important in deeper channels (e.g., Kimmerer et al. 2002). We did a limited amount of sampling across the channel and found no evidence of cross-channel variability in zooplankton (see below), hence we assumed that the point measurements of chlorophyll fluorescence and zooplankton abundance represented the cross-sectional average.

Gross et al. (2009, Equation 18) give all components of salt flux that are expected to be non-trivial in any part of the estuary. Noting that our data include the volume flow rate Q rather than velocity (i.e., integrated over the cross-section), and using their notation with P_c as plankton biomass or abundance in place of S for salt,

$$\text{Total flux} \approx \underset{\text{Advection}}{\langle Q \rangle \langle P_c \rangle} + \underset{\text{Tidal dispersion}}{\langle Q_t P_c \rangle} \quad (1)$$

where brackets indicate averaging over a tidal cycle, and subscript t refers to the tidally varying component of Q, and c refers to quantities that vary with tides but are averaged over the cross-section. The first term in Equation 1 is the advective flux from transport of the mean plankton concentration by the net (tidally averaged) flow, and the second term is the tidal transport from the correlation of tidal flow rate and plankton biomass or abundance.

We calculated tidally averaged flow by applying a low-pass filter to Q to remove variability with a period < ~30 h (Godin 1972), and tidal flow Q_t was the difference between the total flow and the tidally averaged flow. We calculated the phytoplankton flux using the fluorescence data taken at the flux station and calibrated to chlorophyll using 19 samples for extracted chlorophyll taken at the flux station and analyzed as described above. The correlation coefficient between extracted chlorophyll and fluorescence was 0.6. Gaps in the calculated chlorophyll data of up to 1 h were interpolated linearly. Then, we calculated the flux for each day in the time-series when no gap was present by averaging from midnight at the beginning of that day for 24.75 h, close to the tidal day of 24 h 50 min. This removed a small spring-neap periodicity that occurred in data averaged over 24 h.

We collected zooplankton samples every half hour for 26 h beginning around 10 AM on the second day of each sampling period. We used a submersible bilge pump equipped with a calibrated in-line flow meter, which discharged for 20 min into a 150-µm-mesh net. Each sample was preserved with 2–5% formaldehyde, and sub-samples were taken with a target of 100 *P. forbesi* copepodites (actual median copepodites + adults 208, range 101–852) and counted under a dissecting microscope. We converted counts to numbers per m^3 using volume filtered from the flowmeter.

We interpolated flow data from each sampling period to the time-points of the zooplankton samples, and truncated each series at both ends to obtain a series as close as possible to a full tidal cycle. We calculated fluxes separately by life stage and by day vs. night because of obvious differences in life stage between day and night.

The total flux (Equation 1) captures the components of the flux from transport of plankton by the net flow plus the tidal flux from the temporal correlation of abundance with flow. The net flux (first term in Equation 1) was always northward into Liberty Island during this study. Both tidal and net fluxes neglect spatial correlations as discussed above. We expected these to be small because of the shallow, narrow channel, but took 24 of the 51 October zooplankton samples to the east and west of the channel center, alternating among the three positions. We fitted a generalized additive model (GAM) with a spline smoother (function gam in R v. 3.2.3, R development Core Team 2015) to the log-transformed data for adults and copepodites separately. Residuals did not vary by position (east, center, and west) as determined graphically, and confidence intervals for all position parameters overlapped. Therefore, we assumed that the spatial and higher-order terms of the flux were negligible compared with the terms included in Equation 1.

RESULTS

Turbidity was highly variable among stations, and the ratio of depth of the 1% light level to water depth was roughly bimodal, with four of the nine stations having a ratio ~1–2 (Table 1), indicating that the water column was well lit to the bottom. Mean daytime water temperatures across all stations and transects were 22.8°C in June, 24.0°C in July, and 20.5°C in October. Chlorophyll concentrations determined from underway in vivo fluorescence and from filtered samples were generally higher in the northern stations than in the southern stations (Figure 2). Little Holland Tract (HOL) was an exception to this pattern in having low values in July and October. The proportion of extracted chlorophyll >5 µm lacked a clear spatial pattern; monthly mean percentages were 32%, 34%, and 22% for June, July, and October, respectively (Figure 2).

Copepods usually dominated the zooplankton of the CSC, particularly nauplii in the July and October surveys, when a finer-mesh net was used (Figure 3). The calanoid copepod *Pseudodiaptomus forbesi* was usually the most abundant copepod, comprising 88% (median; 10th and 90th percentiles 38–97%) of all post-naupliar copepods, and 91% (53–96%) of the *nauplii*. *Pseudodiaptomus forbesi* adults were relatively uncommon, comprising 5% (1%–17%) of the total post-naupliar stages. This proportion was unrelated to turbidity or to the fraction of the water column that was well lit (Table 1; graphical analysis not shown).

Other copepods were mainly *Limnoithona* spp., other cyclopoids, and a few *Sinocalanus doerrii* and *Eurytemora affinis*. Other taxa (Figure 3) included a variety of cladocera, mainly unidentified species of *Ceriodaphnia* and *Daphnia*, and a snail tentatively

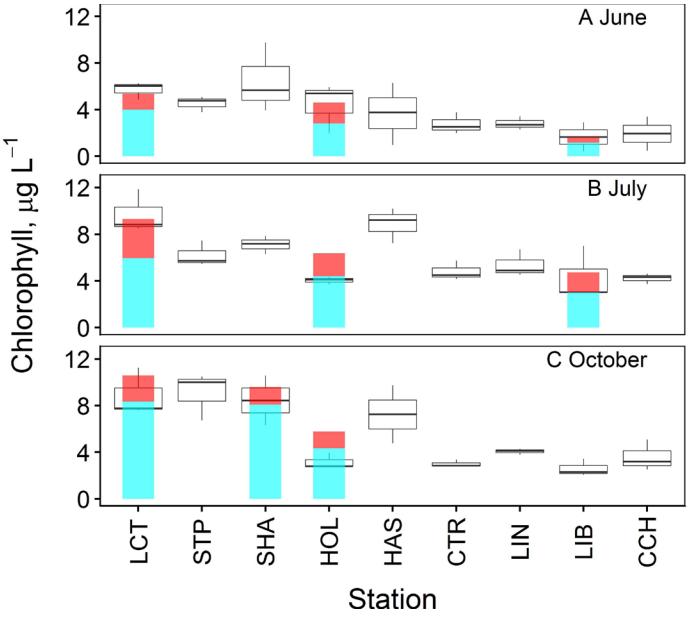

Figure 2 Chlorophyll concentration by station in the Cache Slough Complex (CSC) during June, July, and October 2015. Bars show mean extracted chlorophyll in <5 µm (blue) and >5 µm (orange) size fractions from samples taken at growth-rate stations. Boxplots show chlorophyll at each transect station determined on 3 days per month by in vivo fluorometry calibrated to extracted total chlorophyll.

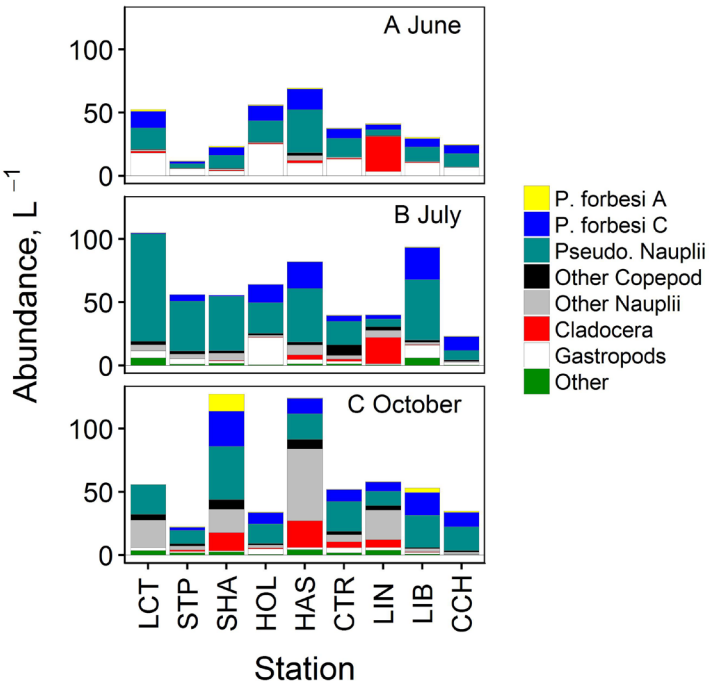

Figure 3 Abundance of major zooplankton groups in samples taken in the Cache Slough Complex (CSC) in June, July, and October 2015. See Figure 1 for station locations. *Pseudodiaptomus forbesi* is shown by stage (A–Adult, C–Copepodite, N–Nauplii) and "Other Copepod" includes both adults and copepodites. Values are means from samples taken on 3 days (2 for CCH and LIB in June). Note that the 150-µm net used in June resulted in lower catches of nauplii than the 53-µm net used in July and October.

https://doi.org/10.15447/sfews.2018v16iss3art4

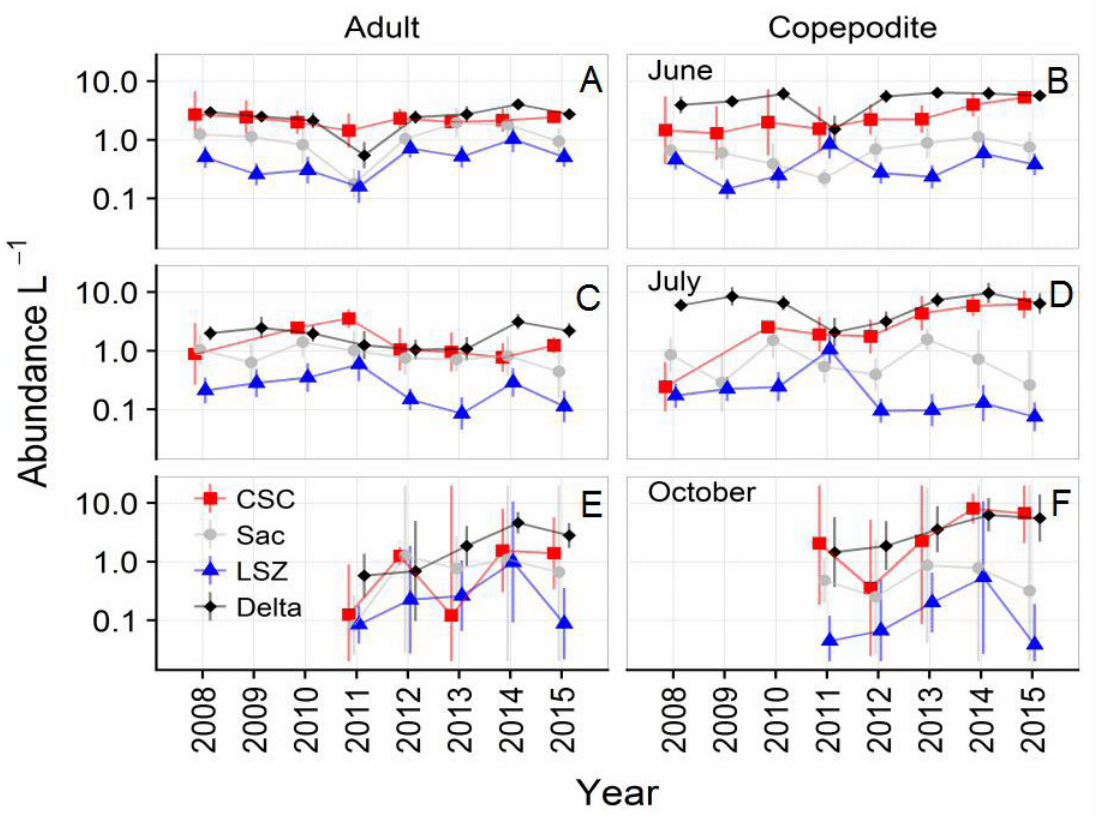

Figure 4 *Pseudodiaptomus forbesi*. Abundance of adults and copepodites from long-term monitoring programs (see Methods) during months sampled in this study in 2015. Data points are geometric mean abundance (10 added to raw data account for zeros) with 95% confidence intervals. Data are grouped by region: Cache Slough Complex (CSC), lower Sacramento River (Sac), low-salinity zone (LSZ, salinity 0.5 to 6, not including stations in the southeast Delta), and the southeast and central Delta.

identified as *Gyraulus* sp. (email from R. Hartman, CDFW, to W. Kimmerer, 2018, unreferenced, see "Notes") that was especially abundant in June.

We used data from long-term monitoring programs to place our results in a broader spatial and temporal context. Abundance of *P. forbesi* from monitoring data was generally highest in the Delta and, on average, nearly as high in the CSC (Figure 4). Abundance was usually lowest in either the lower Sacramento River or the LSZ. In the lower Sacramento River, station 711 at the confluence of the river with Cache Slough had considerably lower abundance than the other stations for both life stages in June and July but not October (not shown). Variability of some data points for October increased (error bars in Figure 4) as a result of lower counts during sample processing.

Abundance of *P. forbesi* copepodites from our study compared well with that from the long-term monitoring programs (Figure 5). However, abundance of adult *P. forbesi* in the southern end of the CSC—that is, near the long-term monitoring stations—was lower in our samples than in the monitoring data in June and especially in July.

Growth and Feeding

Growth rates were well constrained by the calibrated imaging method, with tight clusters of data at each time point of the incubation (Figure 6). In three experiments of nine we cut the analysis off at 2 days' incubation because of a detectable change in growth rate between 0–2 days and 2–3 days (Table 2; examples in Figure 6). This had no apparent effect on the uncertainty in the growth rates. Somatic growth rates of copepods were between 0.23 and 0.53 d^{-1},

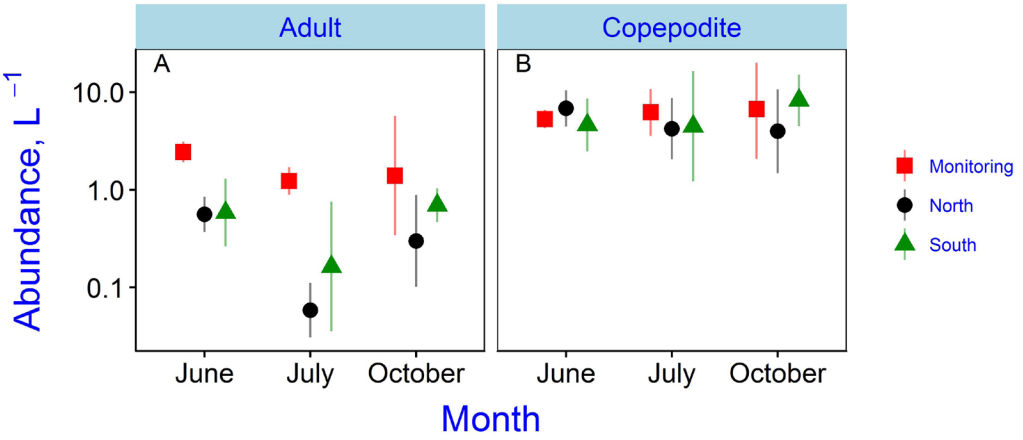

Figure 5 Abundance of *Pseudodiaptomus forbesi* in the Cache Slough Complex (CSC) for adults and copepodites during months of sampling in 2015. "Monitoring" data from CSC in Figure 4; "North", six stations from CTR north; "South", CSC stations CCH, LIB, and LIN, all close to monitoring stations (Figure 1).

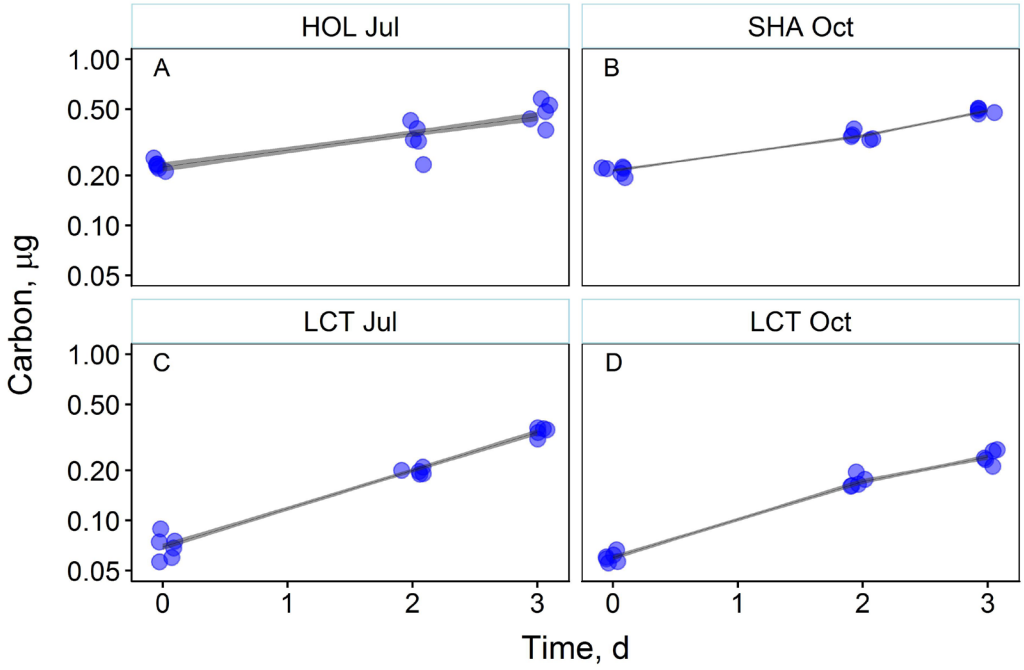

Figure 6 Results of selected growth-rate experiments. Each panel is from a single date and station. Each data point is median carbon per copepod, calculated from volume measured using image analysis on one sample (N=17 to 241, median 35). Specific growth rate is the slope of log carbon per copepod vs. time. Lines give least-squares regression slopes for either 0–3 days or, where slopes changed, for each interval, in which case the first 2-day interval was used to calculate growth rate (Table 2).

and growth rates corrected to 22°C ranged from 0.19 to 0.63 d^{-1} (Table 2). Temperature-corrected growth rates were between 37% and 123% of the maximum rate derived in the laboratory at 22°C of 0.51 d^{-1} (Table 2).

Temperature-corrected growth rates were non-linearly related to chlorophyll concentration and microzooplankton biomass (Figure 7). A rectangular hyperbola for chlorophyll >0.7 µm had a maximum growth rate of 0.5 d^{-1}, a half-saturation constant of 1.6 µg Chl L^{-1}, and a residual standard error of 0.13 d^{-1}. The same parameters for chlorophyll >5 µm were 0.4 d^{-1}, 0.9 µg Chl L^{-1}, and 0.14 d^{-1}—and for microzooplankton biomass they were 0.4 d^{-1}, 1.8 µg C L^{-1}, and 0.13 d^{-1} respectively. The high variability and small number of data points limit the reliability of these parameter estimates.

Using genetic methods to analyze feeding revealed striking differences between the composition of autotrophic plankton in the water and that present in the copepods (Figure 8). Among the major taxonomic groups, relative abundance in the water was highest in cryptophytes and the small cyanobacteria *Synechococcus*, next in ochrophytes (mainly diatoms), lower still in chlorophytes, and small to negligible in other groups. In contrast, copepod samples were high

https://doi.org/10.15447/sfews.2018v16iss3art4

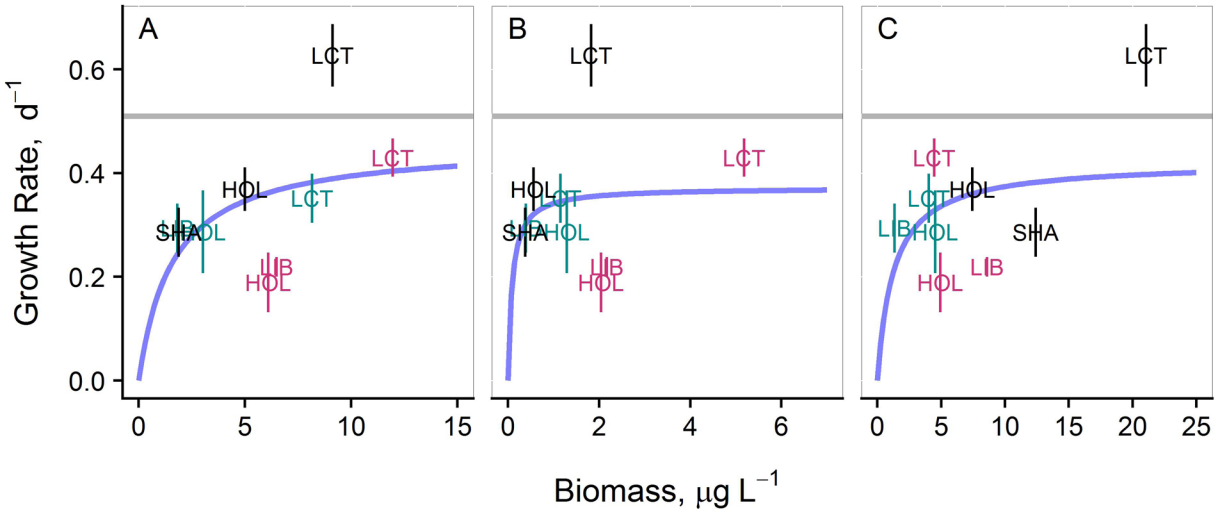

Figure 7 Growth rate plotted against measures of food abundance: (A) chlorophyll concentration (0.7 µm filter, µg L^{-1}); (B) chlorophyll concentration (5-µm filter, µg L^{-1}); (C) microzooplankton biomass (µgC L^{-1}). Growth rates have been adjusted to a temperature of 22 °C using a relationship of egg development time vs. temperature (Sullivan and Kimmerer 2013). Error bars are 95% confidence limits, and the horizontal lines give the laboratory maximum growth rate at 22°C (Kimmerer et al. 2017). Colors indicate months. Curved lines are rectangular hyperbolas fitted to the data (see text).

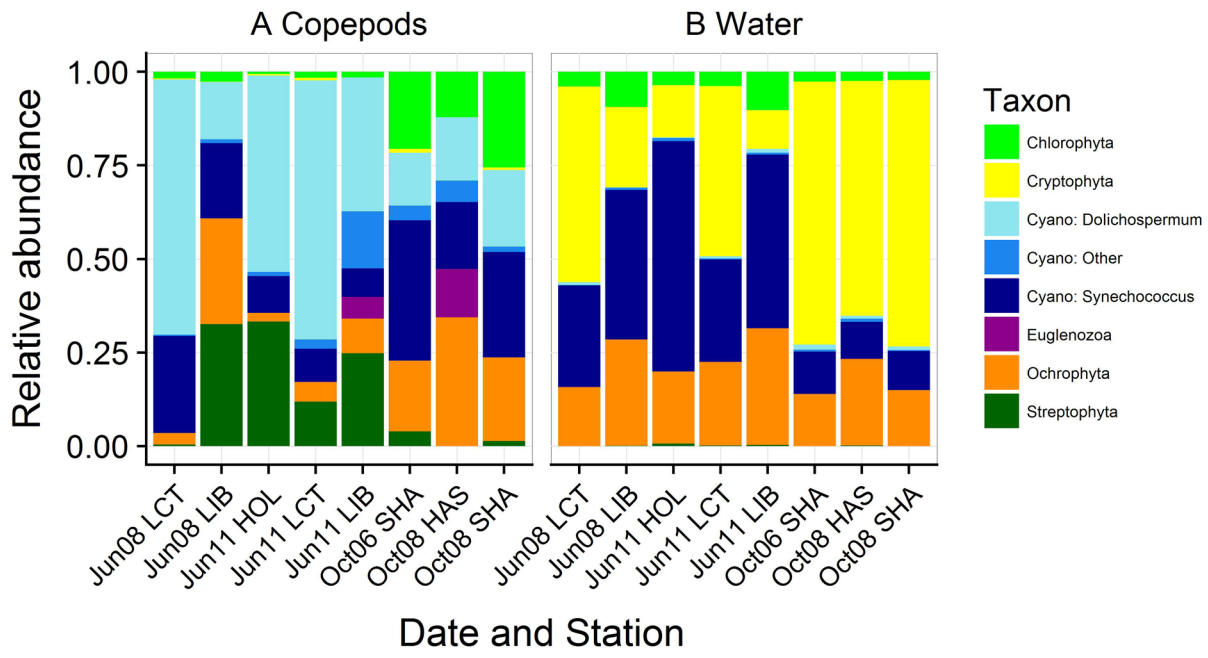

Figure 8 Major phytoplankton groups detected using high-throughput sequencing for samples of copepods (*left panel*) and particulate matter filtered from the water (*right panel*). Data are relative abundance of sequence reads from each group averaged over 12–14 samples of five copepods or two (October) or three (June) particulate samples collected on filters. Sequence reads are expected to be semiquantitative for abundance of each group (Pomanon et al. 2012). Groups are phyla except that cyanobacteria are separated into *Dolichospermum*, *Synechococcus*, and others.

in the cyanobacteria *Dolichospermum* spp. and variably abundant among sampling events in chlorophytes, other cyanobacteria, ochrophytes, and streptophytes. Cryptophyte DNA was nearly absent from the copepod samples (Figure 8).

Stable isotope values for *P. forbesi* showed enrichment of ^{15}N relative to total N in copepods relative to seston, and a slight decrease in carbon isotope ratios ($\delta^{13}C$) between seston and copepods in June only (Figure 9). Shag Slough (SHA), sampled only in October, was an outlier with anomalously ^{13}C-depleted seston relative to other months and stations, and this was reflected in somewhat ^{13}C-depleted copepod samples. Values of $\delta^{15}N$ from copepods exceeded mean values for seston in the same samples by 7.5±0.6, 3.7±1.4, and 5.6±1.7‰ in June, July, and October, respectively (means±95% CI).

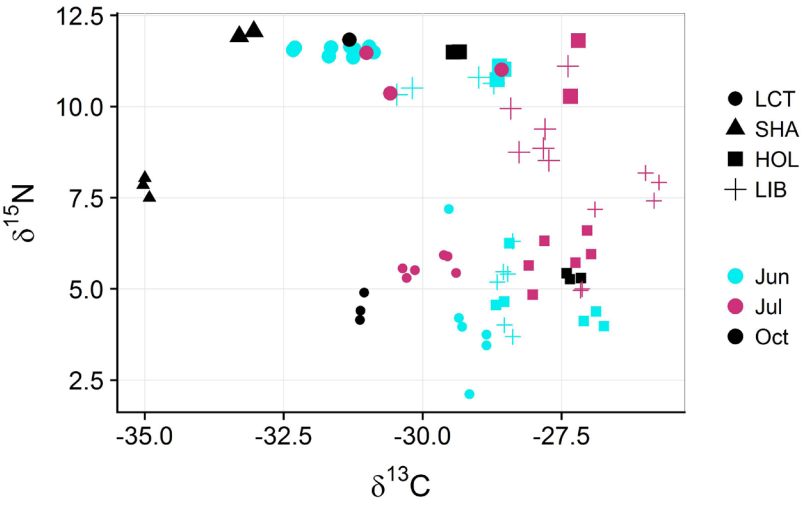

Figure 9 Stable isotope ratios of carbon ($\delta^{13}C$‰) and nitrogen ($\delta^{15}N$‰) of seston collected on filters (small symbols) and *Pseudodiaptomus forbesi* (large symbols). Shapes represent stations (see Figure 1) and colors represent months as in Figure 7.

Flux Study

The chlorophyll flux at station LIB was determined for 127 of the 141 days from June 1 to October 19, 2015. The tidal flux was 0.4±0.6 kg Chl d^{-1}; the net flux was 11.2±0.7 kg Chl d^{-1} (positive into the wetland).

We obtained complete sets of data on *P. forbesi* abundance during all three tidal-cycle studies, including samples taken by day and night on both flood and ebb tides (Figure 10). The most striking pattern in the abundance data was some very high values at night, and very low values by day. Separate relationships of abundance to tidal flow for adults and copepodites (Figure 11) show higher abundance of adults at night than in the daytime, and a less striking day–night difference for copepodites. There was little consistent relationship between direction of tidal flow and abundance, although abundance of adults at night in June was substantially higher on the ebb than on the flood (Figure 11).

The lack of a strong relationship of abundance to tidal flow meant that tidal flux estimates for each month and life stage were generally uncertain and variable (Figure 12). Confidence intervals of tidal flux estimates were smaller

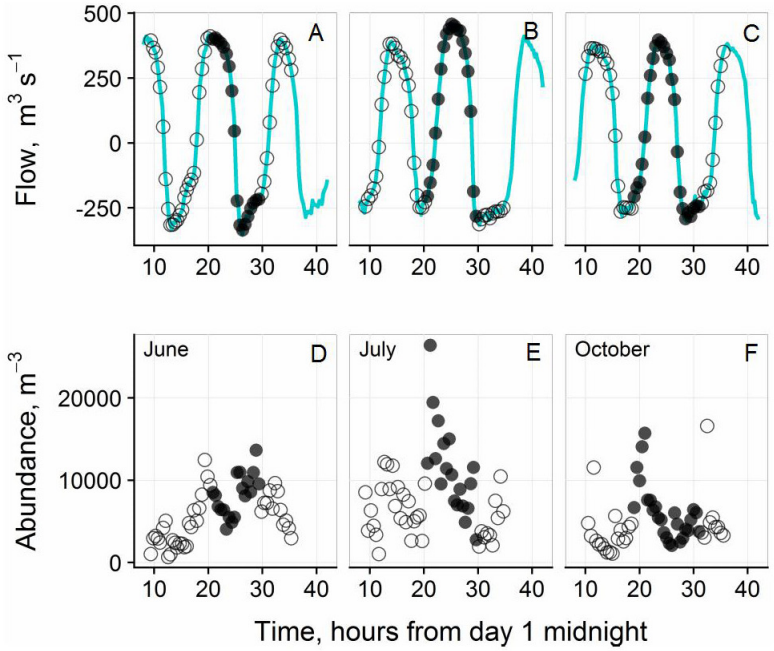

Figure 10 *Pseudodiaptomus forbesi* sampled at the Liberty Island flux station (LIB, Figure 1) during June 9–10, July 20–30, and October 7–8, 2015. *Upper row*, total volume flow rate (Q_t in Equation 1) around the time of the flux studies (positive is landward) with the timing of zooplankton samples indicated by open circles for samples taken by day and filled circles for samples taken by night. *Lower panel*, abundance of total copepodites and adults over time, with symbols as in the upper panel.

https://doi.org/10.15447/sfews.2018v16iss3art4

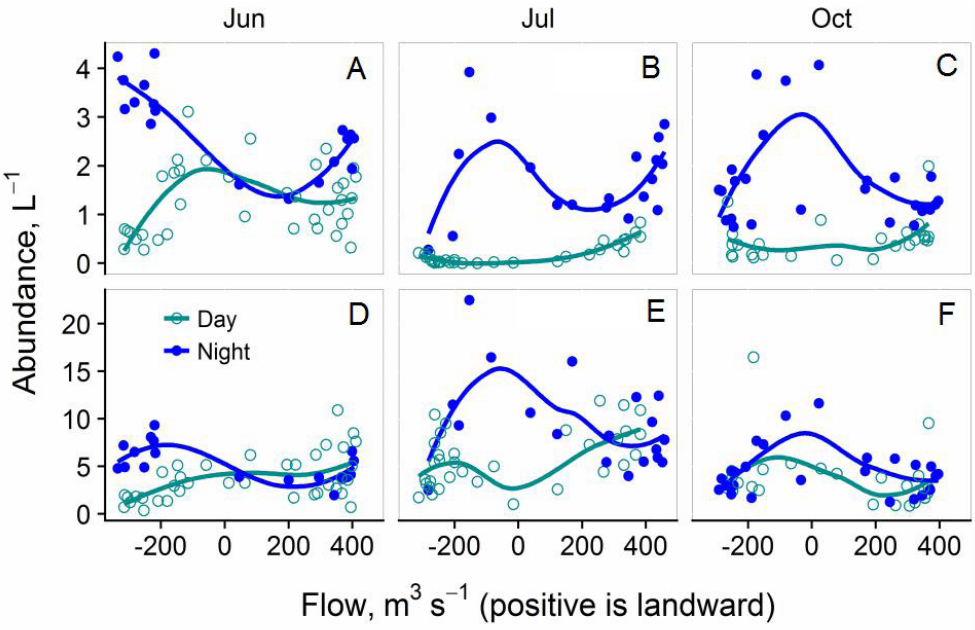

Figure 11 *Pseudodiaptomus forbesi*. Abundance of adults and copepodites vs. total flow through the southern breach of Liberty Island for each 26-hr flux study. Points give abundance of copepods from every sample, and lines are locally weighted regressions (LOESS), both plotted separately for day and night.

by day than by night because of lower daytime variability among individual samples (Figure 11). Means of the daytime values were close to zero, and confidence limits crossed zero except for copepodites in June, for which the flux was positive (into Liberty Island). The night values were similarly variable, with both life stages having negative means in June but with wide confidence limits. Nighttime means for July were greater than zero, although the confidence interval for copepodites barely included zero. The October values were better constrained with negative means but with confidence limits that included zero.

Net fluxes of copepods (not shown) were positive, i.e., into the wetland, for every combination of month, day vs. night, and life stage. Values ranged from 0.04 to 2.0×109 copepods h^{-1}.

DISCUSSION

Much of the interest in wetland restoration in the estuary arises from the value of wetlands as habitat for fishes and other organisms, and their role as productive environments that provide support for food webs throughout the estuary. Plans for restoration or creation of wetlands in the freshwater reaches of the Delta list among their goals the enhancement of food web productivity to support Delta Smelt and other native fishes (e.g., California Natural Resources Agency, undated). This productivity could be made available directly if these fishes occupy the wetlands, or indirect if it is exported in usable form to the open waters of the estuary. In the following sections, we evaluate the roles of the CSC in supporting Delta Smelt directly, and in exporting food for pelagic fishes to the open waters of the estuary.

The Cache Slough Complex as Habitat for Delta Smelt

The CSC appears to be unique among tidal freshwater regions of the estuary in supporting Delta Smelt through their life cycle (Merz et al. 2011; Sommer and Mejia 2013). Some attributes of the CSC indicate that it is poor habitat for Delta Smelt; these attributes include high predator abundance (Sommer and Mejia 2013), high temperature (Komoroske et al. 2015), and toxic contaminants (Weston et al. 2014; Hammock et al. 2015). However, turbidity is generally higher (Morgan–King and Schoellhamer 2013), and abundance of *P. forbesi* was much higher in the CSC than in the LSZ (Figure 4), suggesting better feeding conditions in the CSC. Stomach fullness, RNA:DNA ratios, and glycogen depletion of Delta Smelt indicated good feeding conditions in the CSC in summer 2012–2013, though feeding conditions were apparently better in Suisun Marsh than in the CSC (Hammock et al. 2015).

These results suggest that high food abundance and high turbidity in some regions of the CSC may offset thermal—and possibly contaminant—stress, which may explain the year-round residence of Delta Smelt there. Why are Delta Smelt not abundant in freshwater areas of the Delta outside the CSC? Copepod abundance in these regions is also high (Figure 4), and summer temperature is similar to that in the CSC (Wagner et al. 2011). The Hammock et al. (2015) study was unable to examine freshwater areas outside the CSC, so contaminant effects there are unknown. The virtual absence of Delta Smelt from other freshwater regions of the Delta may result from generally low turbidity there (Nobriga et al. 2008).

Food Web Conditions in the Cache Slough Complex

The relatively high abundance of copepods in the CSC (Figure 4) represents a balance—largely through tidal exchange—among reproduction, mortality, and movement. Put another way, long residence time combined with high productivity can lead to high population densities. Residence time in the northern part of the CSC is probably on the order of a month (Downing et al. 2016). Somatic growth rates of the *P. forbesi* population were high, and although we did not determine reproductive rates, given the high growth rates, they are also likely to be higher than in other parts of the estuary.

Predation on *P. forbesi* in the CSC may not be particularly high. The invertebrate predators that consume early life stages of copepods in the LSZ (Kayfetz and Kimmerer 2017; Kimmerer et al. 2017, 2018) are largely absent from the CSC. The CSC abounds with fish species such as Mississippi Silverside *Menidia audens* and Striped Bass *Morone saxatilis*, but zooplankton comprised a large part of the diet only for Delta Smelt (Whitley and Bollens 2014). However, we have little information on the abundance of invertebrate predators on copepods within the CSC, which could include other copepods and macroinvertebrates such as mysids. Assessing the roles of various predators on copepod abundance would require analysis of reproductive and mortality rates, which were beyond the scope of this study.

The evidence for demersal vertical migration in *P. forbesi* (Figure 11), by which some adults were on the bottom by day, suggests that our study underestimated abundance. This is also suggested by comparing IEP data with our data (Figure 5). The IEP samples were taken by oblique tows, whereas we used subsurface horizontal tows for consistency among stations, and because oblique or vertical tows were not practicable for shallow stations (Table 1). If the copepods were merely deep in the water column and not on the bottom, they would have been vulnerable to the oblique tows but not the horizontal tows.

Copepod abundance at the flux station was highly variable, particularly between day and night (Figures 10 and 11). This variability presumably resulted from the demersal vertical migration of the adult *P. forbesi*, particularly females, which is typical of this widespread estuarine genus (Walter 1987). This behavior is likely an adaptation to risk of visual predation in waters that are shallow or clear enough for fish to see their prey (Fancett and Kimmerer 1985). The abundance of adult *P. forbesi* was also low in nearly all of the samples taken on transects (Figure 3), yet nauplii were very abundant, indicating a large adult population, since reproductive rates of this species are generally low in the estuary (Kimmerer et al. 2014, 2017). Similarly low relative abundance of adults has been observed in other shallow, clear locations (Kimmerer and Slaughter 2016) and is probably the reason for very low adult abundance in parts of the eastern Delta (Kimmerer et al. 2018), including the station eliminated from the means shown in Figure 4 (station 919, see "Methods").

Downing et al. (2016) mapped the distributions of various properties within the CSC during high-speed sampling in October 2014. These included isotope ratios of oxygen and hydrogen in water, from which a measure of water age ("residence time;" Downing et al. 2016) could be determined. Spatial gradients in many properties were apparent, particularly along the north–south axis of the CSC. The northern region of the CSC (near stations SHA, STP, and LCT; Figures 1 and 2) had water ages that exceeded 40 days, and chlorophyll concentrations over 5 µg Chl L^{-1}; chlorophyll concentrations in the southern end of the CSC were 2–3 µg Chl L^{-1}. A similar gradient in chlorophyll concentration was observed in samples taken in May 2014, when ~10–30% of total chlorophyll throughout the CSC was larger than 5 µm (2018 email from F. Wilkerson,

https://doi.org/10.15447/sfews.2018v16iss3art4

SFSU, to W. Kimmerer, unreferenced, see "Notes"). Both the spatial gradient and the low fraction of larger cells are consistent with our results from 2015 (Figure 2). In contrast, cells larger than 5 µm made up ~half of the biomass and productivity in Suisun and San Pablo bays in 2006–2007 (Kimmerer et al. 2012), and larger cells dominate the phytoplankton biomass in San Francisco Bay (Cloern 2018).

The CSC is a mixing zone that links two end-members, the northern CSC – with long residence time, relatively low concentrations of ammonium and nitrate, and relatively high abundance of phytoplankton and zooplankton – and the Sacramento River, with high flow rate and rapid mixing, high inorganic nitrogen concentrations, and low concentrations of most food web constituents. Stations in the northern CSC may be more amenable for population-dynamic studies of copepods than stations in more physically dynamic regions because movement in and out of a habitat can be calculated more readily in regions of higher abundance and therefore steeper gradients (Kimmerer et al. 2018).

Copepod Growth and Feeding in the CSC

Measured growth rates in the CSC were, on average, twice as high as those in the previous studies conducted in estuarine channels (Table 3). Confidence intervals between the CSC data and either earlier data did not overlap. Correcting growth rates to a uniform temperature of 22 °C (Sullivan and Kimmerer 2013) reduced the gap and allowed confidence intervals to overlap among all three studies. This indicates that at least some of the difference in growth rate between this and the earlier studies was caused by higher temperature in the CSC than in the large, open channels of the estuary during this study. However, most of the measured growth rates were lower than the value we determined for this species in the laboratory (Table 2, Figure 7). Although this may be result from, in part, a difference in life stages included in laboratory and field studies, it may also suggest persistent limitation of growth rates in the estuary—even at relatively high biomass of both phytoplankton and microzooplankton (Figure 7). One data point exceeded the maximum growth rate determined in the laboratory for early copepodites (Figure 7); a large fraction of copepods in initial samples from this experiment were nauplii, which grow at a different rate, and this may have biased results high.

Some of the difference in temperature-corrected growth rates among studies (Table 3) is likely from the difference in years and months in which sampling occurred, and none of these studies was designed to compare among years or locations. Part of the problem with conducting such a comparison is the variability among locations and times in the phytoplankton biomass, indexed by chlorophyll, and species and size composition. Size fractionation of chlorophyll in the earlier studies showed that about half of the chlorophyll was >5 µm (Kimmerer et al. 2012, 2017). That size is a rough cut-off for feeding success by particle-feeding copepods (Paffenhöfer 1984), so the >5 µm size fraction is a better measure of food availability than total chlorophyll. A large fraction of the elevated chlorophyll in the northern CSC was in small particles (Figure 2) that were likely not readily available to copepods.

Table 3 Summary of growth-rate estimates for early copepodite stages of *Pseudodiaptomus forbesi* from this study and two previous studies, with 95% confidence intervals (CI), standard deviations (SD), and number of measurements (N). Growth rates presented are those observed at the ambient field temperature and those adjusted to a uniform temperature of 22 °C. Methods are the artificial cohort (AC) method using either carbon mass measured directly or volume calibrated to carbon, and the molt rate method to determine stage durations in the field, coupled with carbon mass by stage.

Years	Months	Method	Locations	Observed growth rate		Growth rate at 22°C		Source
				Mean ± CI	SD (N)	Mean ± CI	SD (N)	
2006–2007	May–July	AC (mass)	LSZ	0.14 ± 0.04	0.07 (12)	0.16 ± 0.05	0.08 (12)	Kimmerer et al. 2014
2010–2012	August–Oct.	Molt Rate	LSZ, Delta	0.18 ± 0.02	0.04 (22)	0.23 ± 0.03	0.06 (22)	Kimmerer et al. 2017
2015	June, July, Oct.	AC (volume)	CSC	0.35 ± 0.09	0.11 (9)	0.34 ± 0.10	0.13 (9)	This study

Nevertheless, both size fractions of chlorophyll and estimated microzooplankton biomass acceptably predicted growth rate in the CSC. The half-saturation constant for chlorophyll was 1.6 µg Chl L^{-1} and that for microzooplankton carbon 1.8 µg L^{-1}, but both were rather poorly constrained by the paucity of data points at low values. Chlorophyll did not predict growth rate in the 2006–2007 studies (Kimmerer et al. 2014), and in 2010–2012 chlorophyll >5 µm predicted growth rate of the late copepod stages of *P. forbesi* but not the early stages examined here (Kimmerer et al. 2017). The poor fit of growth rate to chlorophyll in the earlier studies likely resulted from the persistently low chlorophyll concentrations in those studies, which made both parameters of the growth curve highly uncertain.

The relatively high growth rates seem at odds with the results of the feeding study that used molecular methods (Figure 8). In that study component, which by design detected only autotrophic prey of the copepods, cyanobacteria made up a substantial fraction of the apparent diet, and cryptophytes a negligible fraction, with diatom DNA present in copepods though usually at a lower proportion than in the water (Holmes 2018). Yet, cryptophytes and some diatoms are generally considered highly nutritious foods, and cyanobacteria poor foods, as indicated by differences in essential fatty acids (Burns et al. 2011; Galloway and Winder 2015) and chemical defenses of some cyanobacteria (DeMott and Moxter 1991).

Copepods can generally obtain their nutrition through various selective mechanisms such as selective capture of particles based on size and, possibly, nutritional quality, and differential digestion (Burns et al. 2011). In addition, some cyanobacteria species can provide nutrition for some copepods (DeMott and Moxter 1991; Hogfors et al. 2014). Thus, it is possible that *P. forbesi* was obtaining adequate nutrition through consumption of the chain-forming cyanobacterium *Dolichospermum* spp., despite its capability to produce toxins (Li et al. 2016). Feeding experiments using natural prey in the estuary showed that *P. forbesi* had its highest clearance rates on relatively large diatoms and ciliates (Bouley and Kimmerer 2006; Kayfetz and Kimmerer 2017), but colonial cyanobacteria were not seen in those studies. Feeding experiments at three sites in the Columbia River and its estuary showed moderate to high clearance rates on ciliates and several phytoplankton groups, including cyanobacteria, on one of two sample dates (Bowen et al. 2015).

Consumption of ciliates would not have been detected in the molecular feeding study, and at least some of the small cyanobacteria (*Synechococcus* spp., ~1–2 µm) detected may have been ciliates's food that copepods consumed. These small cells may also have been bound in organic aggregates consumed by the copepods, but we have no information on this process.

The number of samples taken limited the stable isotope data; in particular, the anomalously negative $\delta^{13}C$ in seston from Shag Slough (SHA in Figure 9) was determined in only three samples taken on a single date. Carbon isotopes of copepods generally were more negative than those for seston—except for those from Shag Slough. Stable nitrogen isotope data can be used to infer the trophic position of an organism, because its $\delta^{15}N$ is typically enriched by ~3‰ over that of its food (Peterson et al. 1985). In our study, the $\delta^{15}N$ value of the copepods was elevated about 5‰ above that of the seston (Figure 9). Although seston includes an abundance of particulate matter besides phytoplankton, filtered seston is commonly used to estimate the $\delta^{15}N$ value at the base of the food web (Cloern et al. 2002). This result suggests the presence of an intermediate trophic level between seston and copepods, which also supports the idea that copepods were consuming ciliates that were, in turn, consuming phytoplankton, including cyanobacteria.

Do Wetlands Export Plankton to Open Waters?

Much of the regional interest in restoration of tidal wetlands has focused on the possibility that wetlands could export organic matter, thereby subsidizing food webs in adjacent unproductive pelagic habitats. Wetlands can be major producers of organic matter because of their extensive vegetated surface exposed to sunlight, shallow waters—leading to light penetration through the water column—and the continual supply of nutrients from the open waters and from land (Odum 1980). Even recently restored wetlands are highly productive (Howe and Simenstad 2011). Mass balance ensures that production in

https://doi.org/10.15447/sfews.2018v16iss3art4

excess of respiration by organisms within the wetland must be either buried or exported as organic matter—including organisms—to adjacent estuarine waters.

The "outwelling hypothesis" (Odum 1980; Nixon 1980) holds that the export of organic matter from marshes or estuaries provides an important subsidy to nourish adjacent waters. Demonstrations of its magnitude or importance to estuarine or coastal food webs have been few (Dame et al. 1986; Dame and Allen 1996; Hyndes et al. 2014), and some of the transport may be mediated by mobile organisms such as fish (Kneib 1997). In addition, dissolved and particulate organic matter produced by rooted vegetation can be highly refractory and, therefore, largely unavailable to estuarine pelagic food webs, which may be fueled mainly by phytoplankton (as in the estuary; Sobczak et al. 2002, 2005). Thus, export of phytoplankton or zooplankton would presumably provide a more useful subsidy to pelagic food webs than export of dissolved or detrital organic matter. Because of the potential for high phytoplankton productivity, wetlands could export organic matter as living phytoplankton. However, the extent of this export depends on the geomorphology of the wetland—which influences the proportion of production attributable to phytoplankton (Cohen et al. 2014)—as well as residence time and consumption by benthic grazers, which Lopez et al. (2006) illustrated for flooded islands in the central Delta.

Export of zooplankton from wetlands could provide food to planktivorous fishes in open-water habitats. This export depends on zooplankton behavior and on size- and taxon-specific patterns of mortality. In particular, visual predation by fish in shallow waters can exert strong control on the size distribution, biomass, and species composition of zooplankton (Brooks and Dodson 1965). Vertical movements of zooplankton and hatching or settlement of larvae can lead to spatial patterns of abundance that are inconsistent with passive tidal transport (Houser and Allen 1996). Consumption of zooplankton by small fish that seek food and shelter in shallow areas can reduce zooplankton abundance near shore, and shift the size distribution toward smaller forms, as has been observed in lakes (Brucet et al. 2005, 2010), lagoons (Badosa et al. 2007), and wetlands (Cooper et al. 2012). The outcome can be tidal fluxes into shallow areas (Carlson 1978; Kimmerer and McKinnon 1989), and wetlands can be simultaneously sinks for copepods and areas of aggregation for bottom-oriented larvae (Mazumder et al. 2009). The only previous study of these processes in the estuary found that a marsh at China Camp in San Pablo Bay was a net sink for mysids, probably through predation within the marsh (Dean et al. 2005).

Few studies have examined the specifics of exchange in the wetlands of the estuary. Phytoplankton can be important producers in some wetlands that have extensive areas of open water (Cohen et al. 2014). Nevertheless, food webs in diverse marshes of the estuary are supported more by local plant production than by estuarine phytoplankton (Howe and Simenstad 2007, 2011). The multiplicity of organic-matter sources in wetlands results in distinct pathways of organic matter flow into littoral, wetland, and pelagic food webs (Grimaldo et al. 2009).

Flux Studies in the Cache Slough Complex

The only previously published studies of zooplankton fluxes in the Delta have been at Liberty Island and surrounding wetlands in the CSC (Lehman et al. 2010, 2015). Discrete samples were taken at four stations for chlorophyll concentration (16 occasions) and zooplankton abundance (6 occasions) in 2004–2005, and water flow was calculated from tidal fluctuations in surface elevation and area (Lehman et al. 2010). Fluxes were calculated as the product of hourly flow and the single set of chlorophyll or zooplankton abundance estimates for the month. In 2006, chlorophyll concentration was determined by in situ fluorometry over a single, full tidal cycle, calibrated with chlorophyll concentration from discrete samples. Fluxes were determined as the summed product of concentration and flow (Equation 1). Chlorophyll flux through the southern margin of Liberty Island was negligible (Lehman et al. 2015). Zooplankton flux was variable among months but, based on our results, the variability likely reflects that of zooplankton abundance coupled with the small number of samples taken—in particular, the lack of sampling over the entire tidal cycle.

We obtained similar results to those of Lehman et al. (2010, 2015) with a much higher sampling effort and using flow data from an Acoustic Doppler Current

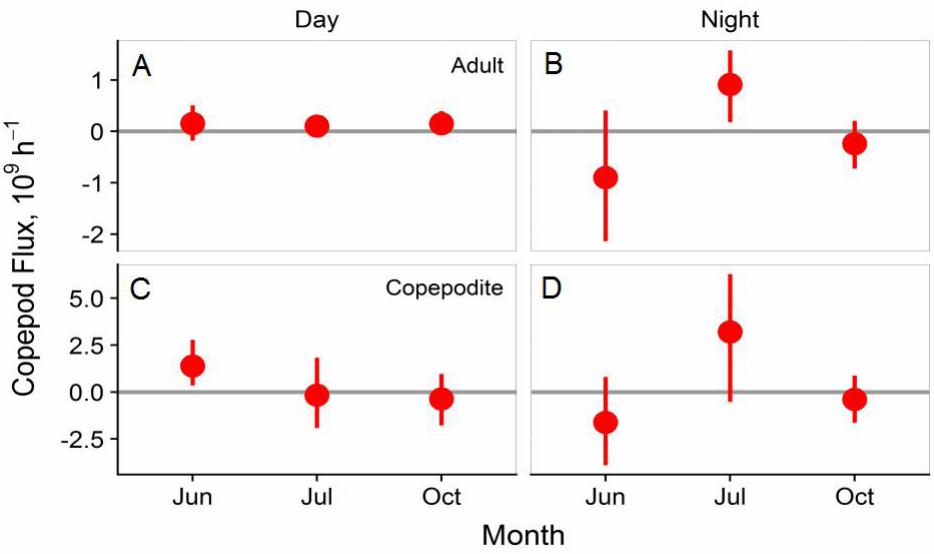

Figure 12 Calculated tidal fluxes of copepods (right-hand term in Equation 1) for *P. forbesi* adults (*top row*) and copepodites (*bottom row*) by day and by night through the southern breach of Liberty Island for each 26-hr flux study. Error bars give 90% confidence limits. Positive values are northward into Liberty Island.

Profiler (ADCP) calibrated to discharge. Chlorophyll flux was determined using a total of >12,000 fluorometric measurements at the ADCP station, yet the daily tidal chlorophyll flux had a long-term mean that was statistically indistinguishable from zero. The mean net chlorophyll flux was northward, or into the wetland, because of the persistent northward net flow of water during this dry period. This was largely a function of imbalances in tidal flow that resulted from numerous levee breaches around Liberty Island; therefore, the tidal flux was a more appropriate measure of the capacity for export than the net flux. Our sampling effort for zooplankton flux included three sampling events of 51 samples each taken near the ADCP. Even at this level of effort, high variability in copepod abundance led to high uncertainty in the flux estimates (Figure 12). In particular, the day–night variability in abundance of adult copepods—presumably from demersal vertical migration—greatly increased this uncertainty.

Despite the high variability, our results indicate no evidence for a persistent tidal flux out of the CSC for either phytoplankton or copepods. Weak spatial gradients and high variability among samples (Figure 10) ensure a low signal-to-noise ratio for estimating fluxes. A better strategy for measuring export fluxes from wetlands may be to conduct such studies in smaller, more confined wetlands where gradients are steep and biological effects such as excess production or consumption in the wetland can be discerned more readily.

ACKNOWLEDGMENTS

Funding was provided by the State and Federal Contractors Water Association under contract 15-11-1 to San Francisco State University, the USGS Western Regional Research program and Cooperative Water program for funding to the USGS, and a STAR fellowship for B. Bemowski at San Francisco State University. Funding for the SFSU MiSeq sequencer was provided by NSF Award #1427772. We thank V. Connor, S. Fong, and K. Cowin for very helpful project management and for facilitating discussions and collaborations with other teams studying the CSC, and M. Weaver for comments that improved the paper. We thank, B. Downing, A. Gorostieta, P. Holliland, T. Johnston, P. Kreun, S. Nagel, K. Nakatsuka, K. O'Donnell, R. Runyon, C. Schmidt, B. Schubert, T. Von Dessonneck, and M. Weaver for help in the field and the laboratory. We also thank F. Cipriano, J. de la Torre, C. Weaver, A. Swei, J. Kwan, B. Chicana, and V. Russell for help with sequencing and bioinformatics.

REFERENCES

Alcaraz M, Saiz E, Calbet A, Trepat I, Broglio E. 2003. Estimating zooplankton biomass through image analysis. Mar Biol 143(2):307-315. *https://doi.org/10.1007/s00227-003-1094-8*

https://doi.org/10.15447/sfews.2018v16iss3art4

Arar EJ, Collins GB. 1997. Method 445.0 In vitro determination of chlorophyll *a* and pheophytin in marine and freshwater algae by fluorescence. [Washington (DC)]: U.S. Environmental Protection Agency, No. EPA/600/R-15/006.

Badosa A, Boix D, Brucet S, Lopez-Flores R, Gascon S, Quintana XD. 2007. Zooplankton taxonomic and size diversity in Mediterranean coastal lagoons (NE Iberian Peninsula): influence of hydrology, nutrient composition, food resource availability and predation. Estuar Coast Shelf Sci 71(1-2):335-346. *https://doi.org/10.1016/j.ecss.2006.08.005*

BDCP: Bay Delta Conservation Plan [Internet]. 2014. California Department of Water Resources. [cited 2018 March 15]. Available from: *http://baydeltaconservationplan.com/*

Bennett WA. 2005. Critical assessment of the Delta Smelt population in the San Francisco Estuary, California. San Franc Estuary Watershed Sci [Internet];3(2). *https://doi.org/0.15447/sfews.2005v3iss2art1*

Bouley P, Kimmerer WJ. 2006. Ecology of a highly abundant, introduced cyclopoid copepod in a temperate estuary. Mar Ecol Progr Ser 324:219-228. *https://doi.org/10.3354/meps324219*

Bowen A, Rollwagen-Bollens G, Bollens SM, Zimmerman J. 2015. Feeding of the invasive copepod *Pseudodiaptomus forbesi* on natural microplankton assemblages within the lower Columbia River. J Plankton Res 37(6):1089-1094. *https://doi.org/10.1093/plankt/fbv078*

Brooks JL, Dodson SI. 1965. Predation, body size, and composition of plankton. Science 150:28-35. *https://doi.org/10.1126/science.150.3692.28*

Brown JH, Gillooly JF, Allen AP, Savage VM, West GB. 2004. Toward a metabolic theory of ecology. Ecology 85(7):1771-1789. *https://doi.org/10.1890/03-9000*

Brucet S, Boix D, Lopez-Flores R, Badosa A, Moreno–Amich R, Quintana XD. 2005. Zooplankton structure and dynamics in permanent and temporary Mediterranean salt marshes: taxon-based and size-based approaches. Arch Hydrobiol 162(4):535-555. *https://doi.org/10.1127/0003-9136/2005/0162-0535*

Brucet S, Boix D, Quintana XD, Jensen E, Nathansen LW, Trochine C, Meerhoff M, Gascon S, Jeppesen E. 2010. Factors influencing zooplankton size structure at contrasting temperatures in coastal shallow lakes: Implications for effects of climate change. Limnol Oceanogr 55(4):1697-1711. *https://doi.org/10.4319/lo.2010.55.4.1697*

Bryant ME, Arnold JD. 2007. Diets of age-0 striped bass in the San Francisco Estuary, 1973-2002. Calif Fish Game 93(1):1-22. *https://www.wildlife.ca.gov/publications/journal/contents#2007*

Burns CW, Brett MT, Schallenberg M. 2011. A comparison of the trophic transfer of fatty acids in freshwater plankton by cladocerans and calanoid copepods. Freshwat Biol 56(5):889-903. *https://doi.org/10.1111/j.1365-2427.2010.02534.x*

CNRA: California Natural Resources Agency. [undated]. Prospect Island tidal habitat restoration project. [cited 2018 February 13]. Available from: *http://resources.ca.gov/docs/ecorestore/projects/Prospect_Island_Tidal_Habitat_Restoration.pdf*

Carlson DM. 1978. Ecological role of zooplankton in a Long Island salt-marsh. Estuaries 1(2):85-92. *https://doi.org/10.2307/1351596*

Cloern JE. 2018. Why large cells dominate estuarine phytoplankton. Limnol Oceanogr 63(S1):S392-S409. *https://doi.org/10.1002/lno.10749*

Cloern JE, Canuel EA, Harris D. 2002. Stable carbon and nitrogen isotope composition of aquatic and terrestrial plants of the San Francisco Bay estuarine system. Limnol Oceanogr 47:713-729. *https://doi.org/10.4319/lo.2002.47.3.0713*

Cloern JE, Jassby AD. 2012. Drivers of change in estuarine-coastal ecosystems: discoveries from four decades of study in San Francisco Bay. Rev Geophys 50:1-33. *https://doi.org/10.1029/2012RG000397*

Cohen RA, Wilkerson FP, Parker AE, Carpenter EJ. 2014. Ecosystem-scale rates of primary production within wetland habitats of the northern San Francisco Estuary. Wetlands 34(4):759-774. *https://doi.org/10.1007/s13157-014-0540-3*

Cooper MJ, Gyekis KF, Uzarski DG. 2012. Edge effects on abiotic conditions, zooplankton, macroinvertebrates, and larval fishes in Great Lakes fringing marshes. J Great Lakes Res 38(1):142-151. https://doi.org/10.1016/j.jglr.2011.12.011

Cordell JR, Bollens SM, Draheim R, Sytsma M. 2008. Asian copepods on the move: recent invasions in the Columbia–Snake river system, USA. ICES J Mar Sci 65:753-758. https://doi.org/10.1093/icesjms/fsm195

Corkett CJ, McLaren IA. 1970. Relationships between development rate of eggs and older stages of copepods. J Mar Biol Assoc UK 50:161-168. https://doi.org/10.1017/S0025315400000680

Dame R, Chrzanowski T, Bildstein K, Kjerfve B, McKellar H, Nelson D, Spurrier J, Stancyk S, Stevenson H, Vernberg J, et al. 1986. The outwelling hypothesis and North Inlet, South Carolina. Mar Ecol Progr Ser 33:217-229. https://doi.org/10.3354/meps033217

Dame RF, Allen DM. 1996. Between estuaries and the sea. J Exp Mar Biol Ecol 200(1-2):169-185. https://doi.org/10.1016/s0022-0981(96)02642-1

Dean AF, Bollens SM, Simenstad C, Cordell J. 2005. Marshes as sources or sinks of an estuarine mysid: demographic patterns and tidal flux of *Neomysis kadiakensis* at China Camp Marsh, San Francisco estuary. Estuar Coast Shelf Sci 63(1-2):1-11. https://doi.org/10.1016/j.ecss.2004.08.019

Dege M, Brown LR. 2004. Effect of outflow on spring and summertime distribution and abundance of larval and juvenile fishes in the upper San Francisco Estuary. In: Feyrer F, Brown LR, Brown RL, Orsi JJ, editors. Early life history of fishes in the San Francisco Estuary and watershed. [Bethesda (MD)]: American Fisheries Society. p. 49-65.

DeMott WR, Moxter F. 1991. Foraging on cyanobacteria by copepods: responses to chemical defenses and resource abundance. Ecology 72(5):1820-1834. https://doi.org/10.2307/1940981

Downing BD, Bergamaschi BA, Kendall C, Kraus TEC, Dennis KJ, Carter JA, Von Dessonneck TS. 2016. Using continuous underway isotope measurements to map water residence time in hydrodynamically complex tidal environments. Environ Sci Technol 50(24):13387-13396. https://doi.org/10.1021/acs.est.6b05745

Fancett MS, Kimmerer WJ. 1985. Vertical migration of the demersal copepod *Pseudodiaptomus* as a means of predator avoidance. J Exp Mar Biol Ecol 88:31-43. https://doi.org/10.1016/0022-0981(85)90199-6

Feyrer F, Nobriga ML, Sommer TR. 2007. Multi-decadal trends for three declining fish species: habitat patterns and mechanisms in the San Francisco Estuary, California, U.S.A. Can J Fish Aquat Sci 64(4):723-734. https://doi.org/10.1139/f07-048

Forster J, Hirst AG, Woodward G. 2011. Growth and development rates have different thermal responses. Am Nat 178(5):668-678. https://doi.org/10.1086/662174

Galloway AWE, Winder M. 2015. Partitioning the relative importance of phylogeny and environmental conditions on phytoplankton fatty acids. PLoS ONE 10(6):e0130053. https://doi.org/10.1371/journal.pone.0130053

Godin G. 1972. The analysis of tides. [Toronto (CA)]: University of Toronto Press.

Grimaldo LF, Stewart AR, Kimmerer W. 2009. Dietary segregation of pelagic and littoral fish assemblages in a highly modified tidal freshwater estuary. Mar Coastal Fish: Dynam Manage Ecosyst Sci 1:200-217. https://doi.org/10.1577/C08-013.1

Hammock BG, Hobbs JA, Slater SB, Acuna S, Teh SJ. 2015. Contaminant and food limitation stress in an endangered estuarine fish. Sci Total Environ 532(0):316-326. https://doi.org/10.1016/j.scitotenv.2015.06.018

Hammock BG, Slater SB, Baxter RD, Fangue NA, Cocherell D, Hennessy A, Kurobe T, Tai CY, Teh SJ. 2017. Foraging and metabolic consequences of semi-anadromy for an endangered estuarine fish. PLoS ONE 12(3). https://doi.org/10.1371/journal.pone.0173497

Herbold B, Baltz DM, Brown L, Grossinger R, Kimmerer W, Lehman P, Simenstad CS, Wilcox C, Nobriga M. 2014. The role of tidal marsh restoration in fish management in the San Francisco Estuary. San Franc Estuary Watershed Sci [Internet];12(1). https://doi.org/10.15447/sfews.2014v12iss1art1

Hobbs JA, Bennett WA, Burton JE. 2006. Assessing nursery habitat quality for native smelts (Osmeridae) in the low-salinity zone of the San Francisco estuary. J Fish Biol 609:907-922. https://doi.org/10.1111/j.1095-8649.2006.01176.x

https://doi.org/10.15447/sfews.2018v16iss3art4

Hogfors H, Motwani NH, Hajdu S, El-Shehawy R, Holmborn T, Vehmaa A, Engstrom-Ost J, Brutemark A, Gorokhova E. 2014. Bloom-forming cyanobacteria support copepod reproduction and development in the Baltic Sea. PLoS ONE 9(11). *https://doi.org/10.1371/journal.pone.0112692*

Holling CS. 1966. The functional response of invertebrate predators to prey density. Mem Entomol Soc Can 98(SupplS48):5-86. *https://doi.org/10.4039/entm9848fv*

Houser DS, Allen DM. 1996. Zooplankton dynamics in an intertidal salt-marsh basin. Estuaries 19(3):659-673. *https://doi.org/10.2307/1352526*

Howe ER, Simenstad CA. 2007. Restoration trajectories and food web linkages in San Francisco Bays estuarine marshes: a manipulative translocation experiment. Mar Ecol Progr Ser 351:65-76. *https://doi.org/10.3354/meps07120*

Howe ER, Simenstad CA. 2011. Isotopic determination of food web origins in restoring and ancient estuarine wetlands of the San Francisco Bay and Delta. Estuaries Coasts 34(3):597-617. *https://doi.org/10.1007/s12237-011-9376-8*

Hyndes GA, Nagelkerken I, McLeod RJ, Connolly RM, Lavery PS, Vanderklift MA. 2014. Mechanisms and ecological role of carbon transfer within coastal seascapes. Biol Rev 89(1):232-254. *https://doi.org/10.1111/brv.12055*

Kayfetz K, Kimmerer W. 2017. Abiotic and biotic controls on the copepod *Pseudodiaptomus forbesi* in the upper San Francisco Estuary. Mar Ecol Progr Ser 581:85-101. *https://doi.org/10.3354/meps12294*

Kimmerer W, Slaughter A. 2016. Fine-scale distributions of zooplankton in the northern San Francisco Estuary. San Franc Estuary Watershed Sci [Internet];14(3). *https://doi.org/10.15447/sfews.2016v14iss3art2*

Kimmerer WJ. 2008. Losses of Sacramento River Chinook Salmon and Delta Smelt to entrainment in water diversions in the Sacramento-San Joaquin Delta. San Franc Estuary Watershed Sci [Internet];6(2). *https://doi.org/10.15447/sfews.2008v6iss2art2*

Kimmerer WJ, Bennett WA, Burau JR. 2002. Persistence of tidally-oriented vertical migration by zooplankton in a temperate estuary. Estuaries 25(3):359-371. *https://doi.org/10.1007/BF02695979*

Kimmerer WJ, Gross ES, Slaughter AM, Durand JD. 2018. Spatial subsidies and local mortality of an estuarine copepod revealed using a box model. Estuaries Coasts *https://doi.org/10.1007/s12237-018-0436-1*

Kimmerer WJ, Hirst AG, Hopcroft RR, McKinnon AD. 2007. Estimating juvenile copepod growth rates: corrections, inter-comparisons and recommendations. Mar Ecol Progr Ser 336:187-202. *https://doi.org/10.3354/meps336187*

Kimmerer WJ, Ignoffo TR, Kayfetz KR, Slaughter AM. 2017. Effects of freshwater flow and phytoplankton biomass on growth, reproduction, and spatial subsidies of the estuarine copepod *Pseudodiaptomus forbesi*. Hydrobiologia 807(1):113-130. *https://doi.org/10.1007/s10750-017-3385-y*

Kimmerer WJ, Ignoffo TR, Slaughter AM, Gould AL. 2014. Food-limited reproduction and growth of three copepod species in the low-salinity zone of the San Francisco Estuary. J Plankton Res 36(3):722– 735. *https://doi.org/10.1093/plankt/fbt128*

Kimmerer WJ, MacWilliams ML, Gross ES. 2013. Variation of fish habitat and extent of the low-salinity zone with freshwater flow in the San Francisco Estuary. San Francisco Estuary Watershed Sci [Internet];11(4). *https://doi.org/10.15447/sfews.2013v11iss4art1*

Kimmerer WJ, McKinnon AD. 1986. Glutaraldehyde fixation to maintain biomass of preserved plankton. J Plankton Res 5:1003-1008. *https://doi.org/10.1093/plankt/8.5.1003*

Kimmerer WJ, McKinnon AD. 1987. Growth, mortality, and secondary production of the copepod *Acartia tranteri* in Westernport Bay, Australia. Limnol Oceanogr 32:14-28. *https://doi.org/10.4319/lo.1987.32.1.0014*

Kimmerer WJ, McKinnon AD. 1989. Zooplankton in a marine bay. III. Evidence for influence of vertebrate predation on distributions of two common copepods. Mar Ecol Progr Ser 53:21-35. *https://doi.org/10.3354/meps053021*

Kimmerer WJ, Parker AE, Lidström U, Carpenter EJ. 2012. Short-term and interannual variability in primary production in the low-salinity zone of the San Francisco Estuary. Estuaries Coasts 35(4):913-929. *https://doi.org/10.1007/s12237-012-9482-2*

Kimmerer WJ, Rose KA. 2018. Individual-based modeling of Delta Smelt population dynamics in the upper San Francisco Estuary III. Effects of entrainment mortality and changes in prey. Trans Am Fish Soc 147(1):223-243. *https://doi.org/10.1002/tafs.10015*

Kimmerer WJ, Thompson JK. 2014. Phytoplankton growth balanced by clam and zooplankton grazing and net transport into the low-salinity zone of the San Francisco Estuary. Estuaries Coasts 37:1202-1218. *https://doi.org/10.1007/s12237-013-9753-6*

Kneib RT. 1997. The role of tidal marshes in the ecology of estuarine nekton. Oceanogr Mar Biol Ann Rev 35:163-220. *https://www.crcpress.com/Oceanography-and-Marine-Biology---An-Annual-Review/book-series/CRCOCEMARBIO*

Komoroske LM, Connon RE, Jeffries KM, Fangue NA. 2015. Linking transcriptional responses to organismal tolerance reveals mechanisms of thermal sensitivity inamesothermal endangered fish. Mol Ecol 24(19):4960-4981. *https://doi.org/10.1111/mec.13373*

Lehman PW, Mayr S, Liu L, Tang A. 2015. Tidal day organic and inorganic material flux of ponds in the Liberty Island freshwater tidal wetland. SpringerPlus 4:273. *https://doi.org/10.1186/s40064-015-1068-6*

Lehman PW, Mayr S, Mecum L, Enright C. 2010. The freshwater tidal wetland Liberty Island, CA, was both a source and sink of inorganic and organic material to the San Francisco Estuary. Aquat Ecol 44(2):359-372. |*https://doi.org/10.1007/s10452-009-9295-y*

Li XC, Dreher TW, Li RH. 2016. An overview of diversity, occurrence, genetics and toxin production of bloom-forming *Dolichospermum* (Anabaena) species. Harmful Algae 54:54-68. *https://doi.org/10.1016/j.hal.2015.10.015*

Lopez CB, Cloern JE, Schraga TS, Little AJ, Lucas LV, Thompson JK, Burau JR. 2006. Ecological values of shallow-water habitats: Implications for the restoration of disturbed ecosystems. Ecosystems 9(3):422-440. *https://doi.org/10.1007/s10021-005-0113-7*

Mazumder D, Saintilan N, Williams RJ. 2009. Zooplankton inputs and outputs in the saltmarsh at Towra Point, Australia. Wetlands Ecol Manage 17(3):225-230. *https://doi.org/10.1007/s11273-008-9102-x*

Merz JE, Hamilton S, Bergman PS, Cavallo B. 2011. Spatial perspective for Delta Smelt: a summary of contemporary survey data. Calif Fish Game 97(4):164-189. *https://nrm.dfg.ca.gov/FileHandler.ashx?DocumentID=46489&inline=1*

Morgan-King TL, Schoellhamer DH. 2013. Suspended-sediment flux and retention in a backwater tidal slough complex near the landward boundary of an estuary. Estuaries Coasts 36(2):300-318. *https://doi.org/10.1007/s12237-012-9574-z*

Moyle PB. 2008. The future of fish in response to large-scale change in the San Francisco Estuary, California. In: McLaughlin KD, editor. Mitigating impacts of natural hazards on fishery ecosystems. p. 357-374.

Moyle PB, Herbold B, Stevens DE, Miller LW. 1992. Life history and status of the Delta Smelt in the Sacramento-San Joaquin Estuary, California. Trans Am Fish Soc 121:67-77. Available from: *https://afspubs.onlinelibrary.wiley.com/doi/abs/10.1577/1548-8659%281992%29121%3C0067%3ALHASOD%3E2.3.CO%3B2*

Nichols F, Cloern J, Luoma S, Peterson D. 1986. The modification of an estuary. Science 231:567-573. *https://doi.org/10.1126/science.231.4738.567*

Nixon S. 1980. Between coastal marshes and coastal waters—a review of twenty years of speculation and research on the role of salt marshes in estuarine productivity and water chemistry. In: Hamilton P, MacDonald K, editors. Estuarine and wetland processes. New York: Plenum. p. 437-525.

Nobriga M, Sommer T, Feyrer F, Fleming K. 2008. Long-term trends in summertime habitat suitability for Delta Smelt, *Hypomesus transpacificus*. San Franc Estuary Watershed Sci [Internet];6(1). *https://doi.org/10.15447/sfews.2008v6iss1art1*

Nobriga ML. 2002. Larval Delta Smelt diet composition and feeding incidence: environmental and ontogenetic influences. Calif Fish Game 88:149-164.

Odum EP. 1980. The status of three ecosystem-level hypotheses regarding salt marsh estuaries: Tidal subsidy, outwelling and detritus-based food chains. In: Kennedy VS, editor. Estuarine perspectives. Academic Press. p. 485-495.

https://doi.org/10.15447/sfews.2018v16iss3art4

Orsi JJ, Walter TC. 1991. *Pseudodiaptomus forbesi* and *P. marinus* (Copepoda: Calanoida), the latest copepod immigrants to California's Sacramento–San Joaquin Estuary. In: Uye S-I, Nishida S, Ho J-S, editors. Proceedings of the fourth international conference on Copepoda. Hiroshima: Bull Plankt Soc Japan. p. 553-562.

Paffenhöfer G-A. 1984. Food ingestion by the marine planktonic copepod *Paracalanus* in relation to abundance and size distribution of food. Mar Biol 80(3):323-333. *https://doi.org/10.1007/bf00392828*

Peterson BJ, Howarth RW, Garritt RH. 1985. Multiple stable isotopes used to trace the flow of organic matter in estuarine food webs. Science 227(4692):1361-1363. *https://doi.org/10.1126/science.227.4692.1361*

Pompanon F, Deagle BE, Symondson WOC, Brown DS, Jarman SN, Taberlet P. 2012. Who is eating what: diet assessment using next generation sequencing. Mol Ecol 21(8):1931-1950. *https://doi.org/10.1111/j.1365-294X.2011.05403.x*

Putt M, Stoecker DK. 1989. An experimentally determined carbon - volume ratio for marine oligotrichous ciliates from estuarine and coastal waters. Limnol Oceanogr 34(6):1097-1103. *https://doi.org/10.4319/lo.1989.34.6.1097*

R Development Core Team. R: A language and environment for statistical computing [Internet]. [cited 2018 October 29] Vienna: R Foundation for Statistical Computing; 2015. Available from: *http://www.R-project.org*

Slater SB, Baxter RD. 2014. Diet, prey selection, and body condition of age-0 Delta Smelt, *Hypomesus transpacificus*, in the upper San Francisco Estuary. San Franc Estuary Watershed Sci [Internet];12(3). *https://doi.org/10.15447/sfews.2014v12iss3art1*

Sobczak WV, Cloern JE, Jassby AD, Cole BE, Schraga TS, Arnsberg A. 2005. Detritus fuels ecosystem metabolism but not metazoan food webs in San Francisco estuary's freshwater Delta. Estuaries 28(1):124-137. *https://doi.org/10.1007/BF02732759*

Sobczak WV, Cloern JE, Jassby AD, Muller-Solger AB. 2002. Bioavailability of organic matter in a highly disturbed estuary: the role of detrital and algal resources. Proc Natl Acad Sci USA 99(scho12):8101-8105. *https://doi.org/ 10.1073/pnas.122614399*

Sommer T, Mejia F. 2013. A place to call home: a synthesis of Delta Smelt habitat in the upper San Francisco Estuary. San Franc Estuary Watershed Sci [Internet];11(2). *https://doi.org/10.15447/sfews.2013v11iss2art4*

Sullivan LJ, Ignoffo TR, Baskerville-Bridges B, Ostrach DJ, Kimmerer WJ. 2016. Prey selection of larval and juvenile planktivorous fish: impacts of introduced prey. Environ Biol Fishes 99(8-9):633-646. *https://doi.org/10.1007/s10641-016-0505-x*

Sullivan LJ, Kimmerer WJ. 2013. Egg development times of *Eurytemora affinis* and *Pseudodiaptomus forbesi* (Copepoda, Calanoida) from the upper San Francisco Estuary with notes on methods. J Plankton Res 35(6):1331-1338. *https://doi.org/10.1093/plankt/fbt076*

Turner JL, Chadwick HK. 1972. Distribution and abundance of young-of-the-year Striped Bass, *Morone saxatilis*, in relation to river flow in the Sacramento–San Joaquin estuary. Trans Am Fish Soc 101:442-452. *https://doi.org/10.1577/1548-8659(1972)101<442:DAAOYS>*

Wagner RW, Stacey M, Brown LR, Dettinger M. 2011. Statistical models of temperature in the Sacramento-San Joaquin Delta under climate-change scenarios and ecological implications. Estuaries Coasts 34(3):544-556. *https://doi.org/10.1007/s12237-010-9369-z*

Walter TC. 1987. Review of the taxonomy and distribution of the demersal copepod genus *Pseudodiaptomus* (*Calanoida*: *Pseudodiaptomidae*) from southern Indo-Pacific waters. Aust J Mar Freshw Res 38:363-396.

Weston DP, Asbell AM, Lesmeister SA, Teh SJ, Lydy MJ. 2014. Urban and agricultural pesticide inputs to a critical habitat for the threatened Delta Smelt (*Hypomesus transpacificus*). Environ Toxicol Chem 33(4):920-929. *https://doi.org/10.1002/etc.2512*

Whitley SN, Bollens SM. 2014. Fish assemblages across a vegetation gradient in a restoring tidal freshwater wetland: diets and potential for resource competition. Environ Biol Fishes:1-16. *https://doi.org/10.1007/s10641-013-0168-9*

Zedler JB, Kercher S. 2005. Wetland resources: Status, trends, ecosystem services, and restorability. Ann Rev Environ Resour 30:39-74. *https://doi.org/10.1146/annurev.energy.30.050504.144248*

NOTES

Hartman, R. 2018. Email communication to W. Kimmerer regarding the tentative identification of snails collected in plankton nets in the Cache Slough Complex.

Howe E, Cordell J, Simenstad C, Smith L. 2016. Trophic ecology of zooplankton and larval fish in the Cache Slough Complex. Poster presented at: 9th Biennial Delta Science Conference; Sacramento, CA.

Khanna S. 2018. Email communication to W. Kimmerer regarding the extent of submerged aquatic vegetation in the Cache Slough Complex.

Wilkerson F. 2018. Email communication to W. Kimmerer regarding chlorophyll concentrations and size-fractionation results in the Cache Slough Complex.

https://doi.org/10.15447/sfews.2018v16iss3art4